AD NUMBER

ADB060787

NEW LIMITATION CHANGE

TO

Approved for public release, distribution unlimited

FROM

Distribution authorized to U.S. Gov't. agencies only; Test and Evaluation; 28 Oct 1981. Other requests shall be referred to Naval Electronic System Command, Washington, DC 20360.

AUTHORITY

DARPA notice, 9 Mar 1988

SCT SYSTEMS CONTROL TECHNOLOGY, INC.
1801 PAGE MILL ROAD □ P.O. BOX 10180 □ PALO ALTO, CALIFORNIA 94303 □ (415) 494-2233

LEVEL II

10 September 1981

Project No. 5364
Task 1 Technical Report, 21 Jul 80-31 Aug 81

59

ANALYSIS OF MISSILE THREAT FOR ADAPTIVE CLOSED-LOOP ELECTRONIC COUNTERMEASURES

Sponsored by:

DEFENSE ADVANCED RESEARCH PROJECTS AGENCY

ARPA Order No. 3613, Amendment No. 4. Program Code No. 0610
Monitored by NAVELEX under Contract No. N0039-80-C-0509
Period of Contract: 21 July 1980 to 31 August 1981
Reporting Period: 21 July 1980 to 31 August 1981

ARPA Order 3613

Approved by:

Stephen M. Rainbolt
Acting Department Manager
Control Technology

Prepared by:

Yair Barniv
Douglas Morgan

"The views and conclusions contained in this document are those of the author and should not be interpreted as representing the official policies, either expressed or implied, of the Defense Advanced Research Projects Agency or the U.S. Government."

This report details the work performed by Systems Control Technology, Inc. (SCT) for Task 1 of contract N00039-80-C-0509. This contract is for the DARPA/NAVELEX Surgical Countermeasures (SCM) program which is directed toward applying observable and control techniques to improve ECM performance. Task 1 of the contract concerns the analysis of the missile threat problem as it impacts the SCM program.

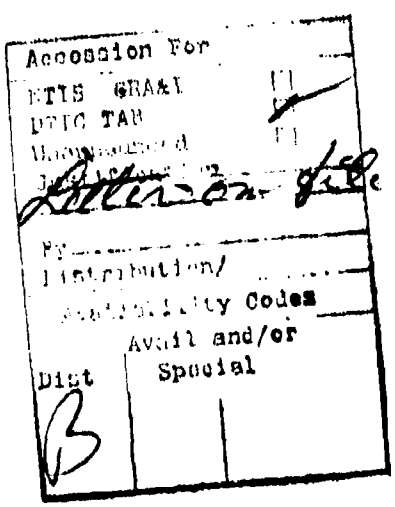

TABLE OF CONTENTS

1. INTRODUCTION

The closed-loop ECM effort has been primarily concerned, up to this point, with inducing a predetermined angular error into the tracking radar of a threatening oncoming missile. This goal is only an intermediate one and has a very limited practical value since it does not directly translate (in a straight-forward manner) to the final "system goal".

The system goal of an ECM carrying target in the case of an attacking missile is to cause that missile to miss by the largest distance possible. Miss distance is therefore the ultimate criterion for an ECM system operating against surface-to-air missiles, cruise missiles or even radar controlled artillery. Adopting this overall performance approach enables one to evaluate any suggested ECM method in the context of a particular target and environment. Moreover, given the scenario, one can synthesize the ECM in a way that will maximize the miss distance.

One of the most important constituents of the scenario is the type of ECM carrying target to be protected. The two main targets of concern are ships and aircraft, and the corresponding ECM methods and analysis seem to be entirely different. The case of a high-altitude aircraft is clearly three-dimensional (3-D) while the case of a ship is, in many cases, 2-D only. More important, an aircraft can be thought of as a point target and the miss distance can be simply measured from its center, whereas the definition of a miss distance for a ship is not so obvious. Because of these and other essential differences, we intend to deal with each target case separately, and to concentrate in the present work on the aircraft target case only.

List of Notations

$R(t)$ - instantaneous target/missile range.

R_0 - initial target/missile range.

t - time from the beginning of the interception.

t_1 - time of disturbance application from the beginning of the interception.

τ - time-to-go to collision.

T - normalised time-to-go- $\omega_0 \tau$.

T_f - total interception time.

T_{sw} - period of memory homing after breaking track.

s - Laplace transform variable.

V_t - target velocity.

V_m - missile velocity.

V_c - relative target/missile closing velocity.

A - aspect angle: angle between V_t and the LOS; also amplitude of the circular disturbance.

L - lead angle: angle between V_m and the LOS.

ψ - track crossing angle; also absolute phase of the circular ECM disturbance.

γ - heading launch error or absolute angle of V_m in space.

λ - the LOS angle in space; also normalized s , s/ω_o.

λ_D - general 1 - D disturbance angle.

λ_p, λ_y - pitch or yaw components of the 2-D LOS disturbance angle.

λ_{max} - upper bound on the controlling λ_D .

ε - seeker's error.

θ_h - seeker's gimbal angle.

θ_m - missile's pitch angle with respect to space.

Y_t - target displacement perpendicular to the LOS.

$\overline{Y_t}$ - a unit step input of disturbance in Y_t .

$\delta Y_t(t-t_1)$ - an impulse disturbance of Y_t applied at t_1 in the forward system.

$\delta(\tau)$ - an impulse applied to the adjoint system to initiate the run backwards from the collision time $\tau = 0$.

Y_m - missile displacement perpendicular to the LOS.

ΔY - relative target/missile displacement.

N - proportional navigation constant.

m - miss distance in general.

m_C - the circular-orbit overall (2-D) miss for a one rad disturbance amplitude.

m_{CB} - the maximum bounded m_C .

m_y, m_p - the yaw and pitch components of m_c .

m_{max} - the 1-D optimal-control miss for a ± 1 rad disturbance.

m_B - the bounded 1-D optimal-control miss.

$m(\tau)$ - the function relating the miss with the time-to-go.

$m(\tau)/\_\overline{Y_t}$ - $m(\tau)$ resulting from a Y_t step.

$m(\tau)/(*)$ - same as above for a general type of disturbance.

$W(t)$ or $W(\tau)$ and $W(s)$ - the impulse-response (same in the forward or the adjoint systems) and the Laplace-transform of the time-invariant function representing the antenna, AP, and aerodynamics of the missile.

$H(\tau)$ - the adjoint system feedback quantity.

G - the seeker's open-loop transfer-function.

τ_1, τ_2 - time constants of the seeker.

k - open-loop seeker's gain.

τ_M - time-constant of the memory circuit.

τ_{AP} - time-constant of the AP.

ω_0, ϕ - frequency and phase (with respect to collision) of the circular ECM disturbance.

sw1, sw3 - switches which are open only during the memory period T_{sw} before collision

sw2 - inverse of sw1.

a_C	- acceleration command
a_{CM}	- filtered acceleration command
AP	- Auto-Pilot
BT	- Break-Track
LOS	- Line-of-Sight between the missile and the target
MD	- Miss-Distance
IC	- Initial Condition
Eq. (*.*) or (*.*)	- indicates an equation number
OC	- Optimal Control
CO	- Circular Orbit

2. THE INTERCEPTION MODEL

The scenario to be analyzed here is that of an ECM equipped aircraft which tries to defeat a homing missile. The worst case for the aircraft is to fly high (so that there is no hope of driving the missile into the ground) and towards the missile's launching site (so that the available time for evasion is the minimum). The missile carries an active or a passive radar and the ECM effect shows up through an induced additive angular error.

The aircraft is assumed to have some prior knowledge and real time observables regarding the missile. The effect of these on the ECM performance will be discussed later, except for one assumption, regarding the missile's roll stabilization, that has to be made at the outset. The assumption to be made here is that the missile's pitch and yaw dynamics are isolated through the employment of roll stabilization or an effective roll damping (a steady roll rate is acceptable). This assumption is essential to the missile's designer himself in order to ensure good performance so that there is no loss of generality from the ECM designer's viewpoint.

The pitch/yaw separation assumption allows one to analyze a planar (2-D) instead of a 3-D problem. Figure 2.1 shows the planar geometry of homing in either the Pitch or the Yaw planes; this geometry is often referred to as "the collision triangle" because it describes the steady-state geometry leading to collision. The target has a velocity V_t and the interceptor has V_m. If the target does not accelerate, the initial range, R_o, and the angle L between the velocity vector, V_m, and the LOS determine the proper course (lead angle L relative to LOS) and time of flight, T_f, to collision for the interceptor. A is called the aspect angle and ψ is the track crossing angle. The law of sines determines the lead angle and the law of cosines determines the relative velocity and hence the flight time T_f, thus ideally:

$$V_m \sin L = V_t \sin A \tag{2.1}$$

$$V_c = V_m \cos L + V_t \cos A \tag{2.2}$$

$$T_f = R_o/V_c \quad . \tag{2.3}$$

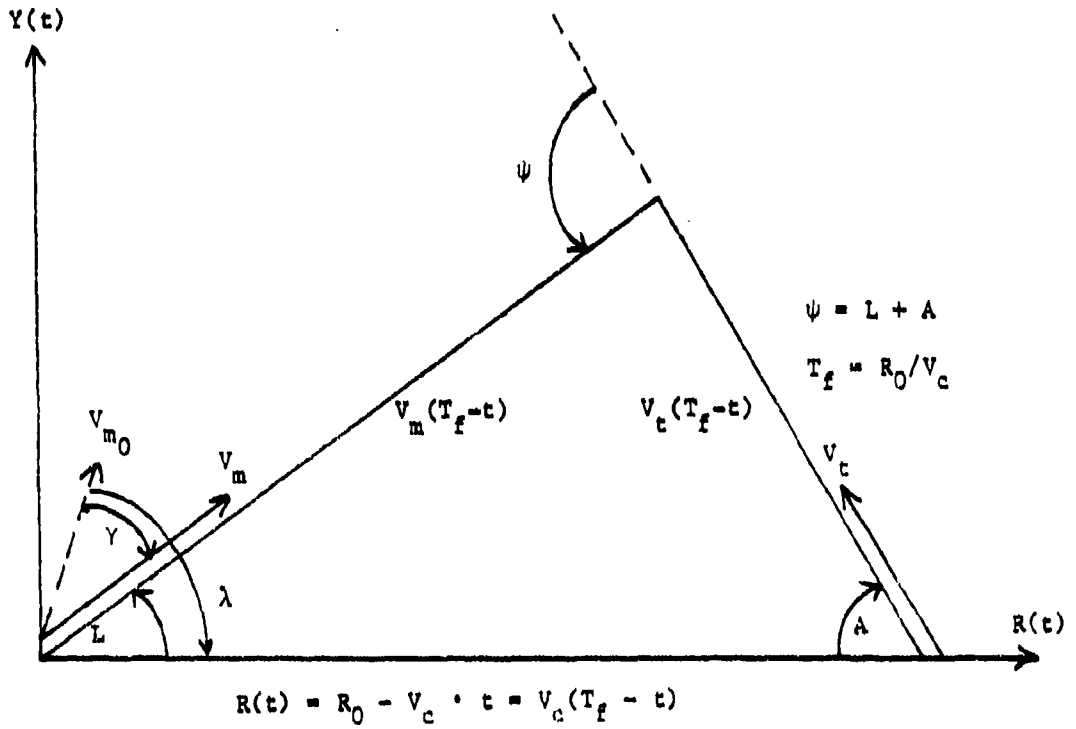

Fig. 2.1 The Homing Collision Triangle

At the beginning of interception the interceptor's velocity vector points (in general) to the wrong direction. The dotted vector V_{m_o} makes an angle γ with the proper course, where γ is referred to as the heading launch error (V_{m_o} also serves here as the reference direction in space and is assumed to lie in the collision plane).

The commonly used next step to be taken for analysis is to linearize the problem by applying small perturbations to the collision triangle parameters. One is interested in obtaining the incremental λ (the angle of the LOS in space) due to increments of target and missile displacements Y_t and Y_m, perpendicular to the range vector. It is simple to realize that one can circumvent this procedure by collapsing the collision triangle to where the small angle convention holds for L and A (the result for the general case will be given shortly). This is virtually a head-on intercept which can be described by Fig. 2.2. In this figure Y_t, Y_m and λ are the perturbations or their corresponding absolute values (the same notation is used for both), i.e. (see Fig. 2.1):

$$Y_t = V_t \sin A\, t$$

$$Y_m = V_m \sin L\, t \qquad (2.4)$$

$$R(t) = R_o - V_c\, t \quad .$$

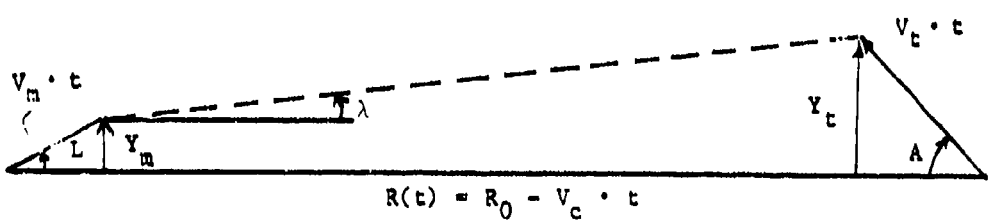

Fig. 2.2 The Linearized Interception Geometry

The equation for the perturbation λ can then be simply written as

$$\lambda \cong \frac{Y_t - Y_m}{V_c(T_f - t)} \quad ; \quad V_c \cong V_m + V_t \tag{2.5}$$

Before proceeding any further, we intend to present (see Fig. 2.4) a typical block diagram [1] of the homing closed-loop, and to simplify it in steps so as to elaborate on the above basic relationships and delineate the way to proceed with the analysis. The 2-D block diagram of Fig. 2.4 is based on the angular relationships shown in Fig. 2.3.

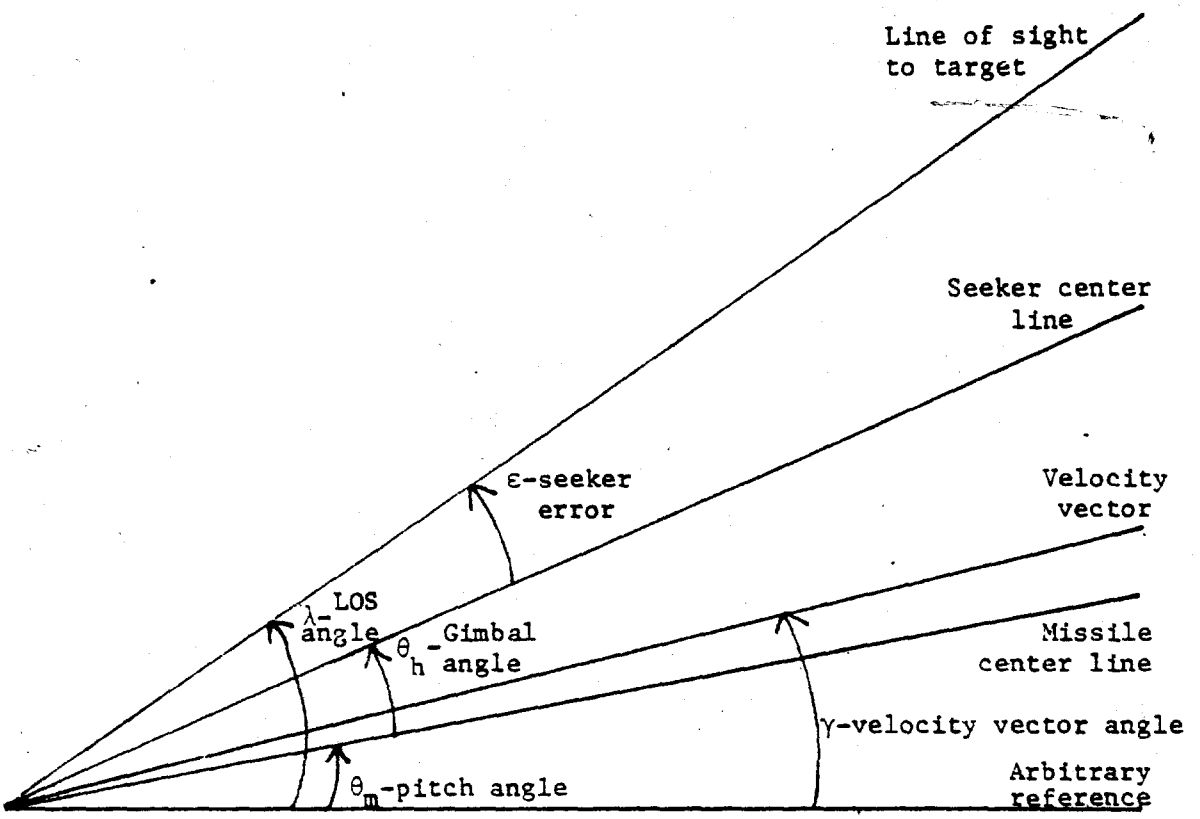

Fig. 2.3 The Basic Angles Involved in the Homing Geometry

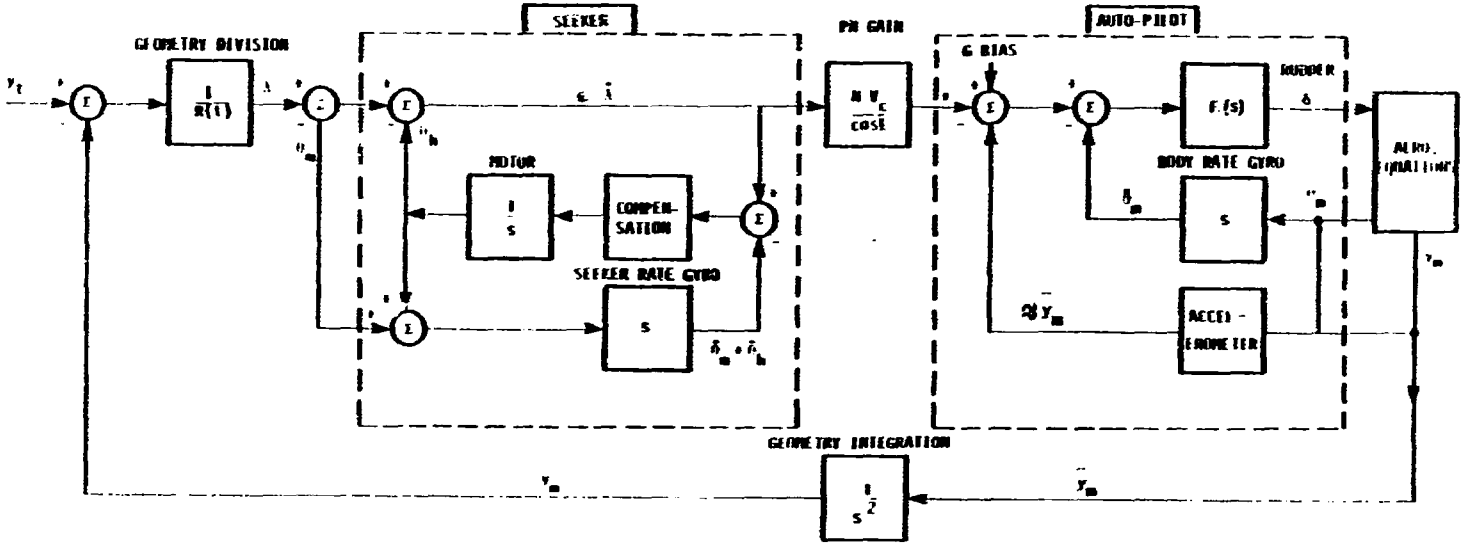

Figure 2.4 The Homing Closed-Loop Diagram for the Pitch or Yaw Planes

The relationship for the seeker error obtained from Fig. 2.3 by inspection is:

$$\varepsilon = \lambda - \theta_h - \theta_m \quad , \tag{2.6}$$

where the four angles involved are defined in the figure itself. The angle λ in Fig. 2.4 is given by Eq. (2.5), where Y_t and Y_m can either represent absolute or perturbation quantities. The reason why both view points are interchangeable is that the quantities used for control, either θ_h (for pursuit navigation) or $\dot{\lambda}$ (for proportional nav.) are independent of the chosen reference coordinate system. The seeker's control (which comprises the blocks inside the left broken-line frame) is designed so that the error, ε, represents $\dot{\lambda}$ for frequencies within the relevant bandwidth. The 1/s block represents the electrical (or hydraulic or pneumatic) motor which drives the antenna to the angle θ_h with respect to the missile's body. The s block represents a rate-gyro which serves to isolate the antenna direction in space from the missile's body maneuvers.

The error $\varepsilon \approx \dot{\lambda}$ serves in the implementation of the proportional navigation law, where one is interested in controlling the missile's acceleration perpendicular to the LOS to be:

$$\ddot{Y}_m = N V_c \dot{\lambda} \quad . \tag{2.7}$$

The commanded acceleration at the input to the Auto-Pilot (AP) must, in general, be 1/cosL larger since the AP can only exert acceleration perpendicular to the velocity vector (can cause $\dot{\gamma}$).

It turns out that the factor 1/cosL (which is essentially a constant) makes the only difference (in the diagram of Fig. 2.4) between the general case shown in Fig. 2.1 and the head-on case shown in Fig. 2.2. In order to realize (2.7) (assuming $L \approx 0$ for the rest of this work), $N V_c \dot{\lambda}$ is applied (along with a g - bias, if in the vertical plane, to compensate for gravity) to the AP which is essentially an acceleration feedback closed loop. The AP output is a rudder angle, and the relevant quantity for homing is $\ddot{Y}_m$ which is related to the rudder angle through the aerodynamical equations. The homing loop is finally closed by the missile displacement, Y_m, (perpendicular to the LOS) which is the result of the double geometrical integration.

At this point, it is noteworthy to indicate that in a 6 degrees of freedom simulation, two channels similar to Fig. 2.4 are used. The two seeker errors, ε_y and ε_p, in azimuth and in elevation are derived by transforming the 3-D vector $\left|X_t - X_m\ ,\ Y_t - Y_m\ ,\ Z_t - Z_m\right|$ through the body/earth and seeker/body transformations (matrices), where $\left|X_t\ ,\ Y_t\ ,\ Z_t\right|$ and $\left|X_m\ ,\ Y_m\ ,\ Z_m\right|$ are the absolute location vectors of the target and the missile respectively; notice that this double transformation replaces the 2-D geometry given by (2.6).

The next step we make is to simplify the diagram of Figure 2.4 to that of Fig. 2.5. The block G in Fig. 2.5 represents the "Transfer-Function", $\theta_h/\dot{\lambda}$, which includes the 1/s, s, and the compensation block appearing in the seeker part of Fig. 2.4. Notice that an ideal seeker space-stabilization against a θ_m input is assumed so that θ_m plays no further role and does not show up in Fig. 2.5. Also, it is important to indicate that G includes one integration so that the approximation $\varepsilon \simeq \dot{\lambda}$ still holds. Another impressive short-cut made in this simplification is to reduce the whole AP and aerodynamics into a single first order pole. Although this step appears to be somewhat simplistic at first glance, it is nevertheless reasonable to make since the function of a well-designed AP is to yield an almost constant closed-loop response in spite of large plant (aerodynamics) variations. A practical way to estimate the equivalent overall time-constant, τ_{AP}, is to fit the Bode curves of a 1-pole and the closed-loop AP responses.

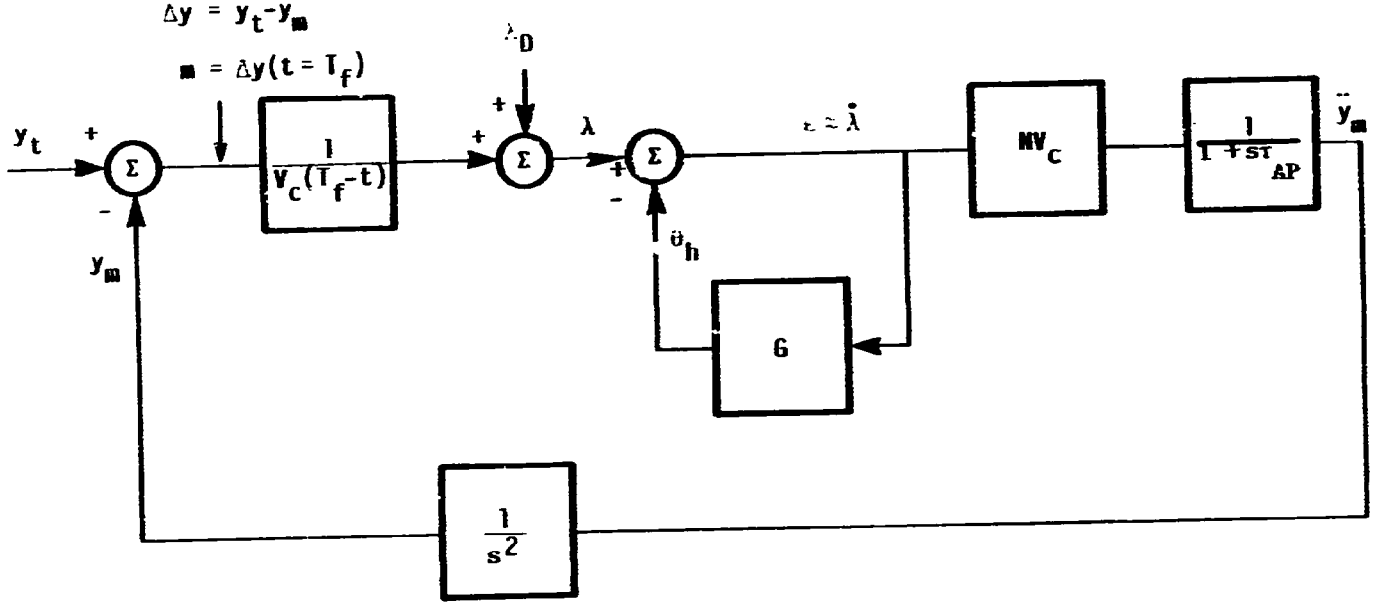

Figure 2.5 A Simplified Block Diagram of the Homing Loop

3. THE APPLICATION OF THE ADJOINT METHOD TO THE MISS-DISTANCE CALCULATION

The Adjoint Method can be used to reduce the analysis of a terminal value linear time-varying problem to a one-variable (miss-distance) impulse-response problem which is (in our case) Laplace transformable [2]. The method can be explained with the help of Fig. 3.1. Fig. 3.1a shows four typical graphs of the quantity $\Delta y(t,t_1) = Y_t - Y_m$ (appearing in Fig. 2.5) as a function of time, t, where each graph represents the response to a target displacement step input, $\sqrt{Y_t}$, (initially $Y_t = Y_m = 0$) applied at different times $t_1 < T_f$. All graphs are terminated at $t = T_f$ which is the common time of collision. The value of Δy at that instant is defined as the miss distance, m, resulting from a disturbance applied at t_1, i.e.,:

$$m = \Delta y(T_f, t_1) \quad .$$

Notice that, if the input step is applied a long time before collision, the Homing loop succeeds in decaying the resulting miss to a small value, m_1. On the other hand, if the target "jumped" at the last moment (just before collision), it is obvious that the missile has no time to make any correction; thus the miss then equals the full input step size ($m_5 = 1$) .

Fig. 3.1b summarizes the miss-distance results of all possible (infinite) runs of the type shown in Fig. 3.1a in a single continuous graph. This graph is the miss as a direct function of the net flight time, τ, (from the application of the disturbance at $t = t_1$ to collision at $t = T_f$). Notice that t_1 and T_f are absolute times, counted from an arbitrary instant $t = 0$, while τ is the time-to-go to collision; thus, τ may take any positive value. The $\sqrt{Y_t}$ at the denominator of m(t) symbolizes the fact that this is the miss distance resulting from a unit-step input of Y_t.

The Adjoint Method enables one to obtain graphs of the type shown in Fig. 3.1b in a single run.

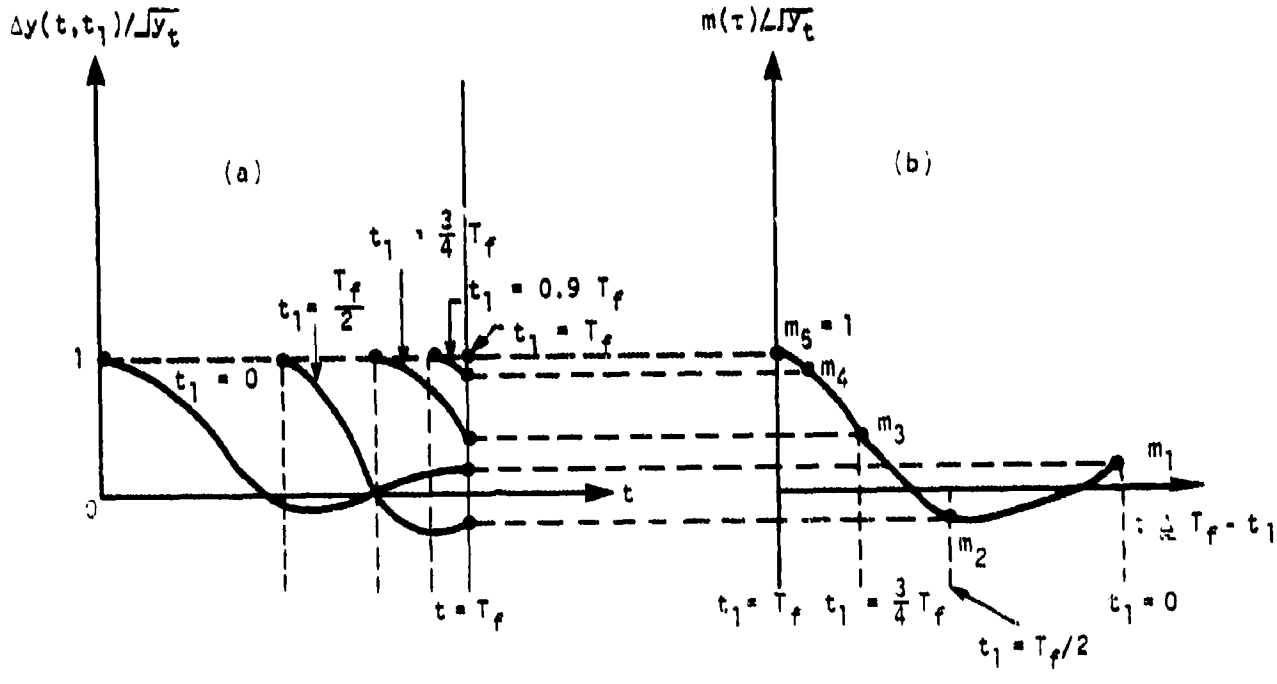

Figure 3.1 The Relationship Between the Original (a) and the Adjoint System (b) Responses

It involves the construction of an "adjoint system" according to a theory and a set of rules which can be found in many works (such as [1, 2, 3])

As an example, we will further simplify Fig. 2.5 by reducing the antenna, AP and Aerodynamics into a single time invariant operator (having an impulse response W(t)) as shown in Fig. 3.2.

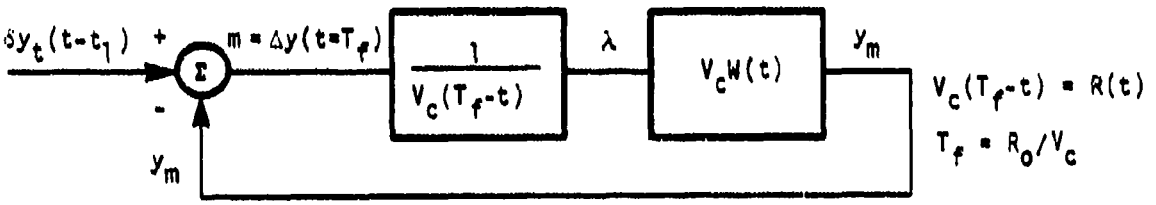

Figure 3.2 A Simplified Homing Loop Subjected to an Impulse of Target Displacement, δy_t, Applied at t_1 ($T_f - t_1$ Before Collision)

In this figure the Homing loop is subjected to an impulse of target displacement only (no other disturbances exist). The adjoint system, corresponding to the above, is shown in Fig. 3.3, where the miss, $m(\tau)$, is now a function of the "time-to-go", $\tau = T_f - t_1$, and $\delta(\tau)$

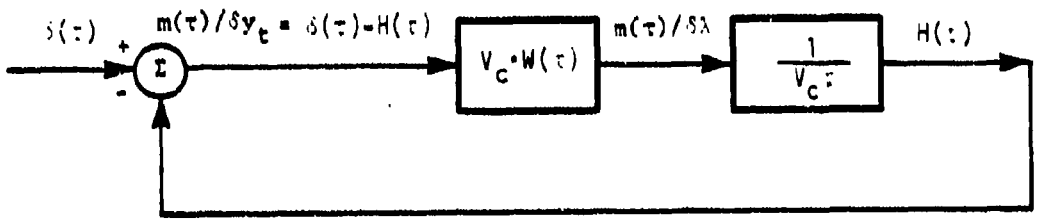

Figure 3.3 The Adjoint System Corresponding to the Homing Loop Shown in Figure 3.2.

is an impulse applied at $\tau = 0$ which drives the system from the collision instant backwards. It is seen from the Figure that

$$m(\tau)/\delta y_t = \delta(\tau) - H(\tau) \quad , \tag{3.1}$$

and $H(\tau)$ can be expressed through the convolution principle as

$$H(\tau) = \frac{1}{\tau} \int_0^\infty W(x) \, [\delta(\tau-x) - H(\tau-x)] \, dx \quad . \tag{3.2}$$

One can now Laplace transform both sides of (3.2) (since τ is defined in the range $0 \to \infty$ which is not the case for t in the original system) and obtain:

$$-\frac{dH}{ds} = W(1-H)$$

or

$$\frac{d}{ds}(1-H) = W(1-H) \quad . \tag{3.3}$$

The last result makes use of the following relationship regarding the Laplace Transform.

$$\mathcal{L}[\tau \cdot H(\tau)] = -dH(s)/ds \quad .$$

Integrating in the s domain, we have:

$$\int \frac{d(1-H)}{1-H} = \ln(1-H) = \int W ds + k \; ;$$

$$1-H = C \exp\left[\int W ds\right] = \mathcal{L}\left[\frac{m(\tau)}{\delta y_t}\right] \quad , \tag{3.4}$$

where the last relationship is obtained from (3.1).

The constant C can now be found using the fact that the miss distance due to a step in target displacement (not an impulse), which occurred just prior to collision, equals unity; thus:

$$m(o)/\sqrt{Y_t} \triangleq 1 = \lim_{s \to \infty} s\left(\frac{1-H}{s}\right) = \lim_{s \to \infty} C \exp\left[\int W ds\right] \quad . \tag{3.5}$$

Eqs. (3.1), (3.4) and (3.5) provide an analytic solution for 1-H (and thus for the miss distance) in some special cases of W . For example:

$$W = \frac{N}{s(s/\omega_o+1)} \rightarrow 1-H = \left(\frac{s/\omega_o}{s/\omega_o+1}\right)^N \quad , \tag{3.6}$$

and the miss distance for a step of target acceleration (with $N = 3$) is

$$m(T)/\sqrt{a_t} = \mathcal{L}^{-1}\left[\frac{\lambda^3}{s^3(\lambda+1)^3}\right] = \frac{T^2}{2\omega_o^2}\exp(-T) \quad , \tag{3.7}$$

where $T = \omega_o\tau$ and $\lambda = s/\omega_o$ are used for normalization. The gain of $N = 3$ in W of (3.6) can be identified as the proportional navigation constant (appearing in Fig. 2.5) and is the minimum value which will yield a converging miss distance for an accelerating target as is obvious from (3.7).

It is important to realize that an analytic result can always be obtained for any $W(t)$ in the system of Fig. 3.2 by formally solving (3.4). The general solution is, however, extremely unmanageable except for some few specific cases such as that of (3.6). In other words, running a digital simulation of the Adjoint System is far simpler than numerically evaluating the result of (3.4) in the general case. Once adopting this approach, there is no limit on the complexity of the homing loop, as long as it can be considered a linear, time-varying system.

4. ECM APPLIED TO THE HOMING MISSILE

In all practical cases of homing missiles there is a minimum range at which the sensor becomes "blind", and no further measurements are possible. In the case of controlled ECM it is possible to break track at a range much larger than the regular blind range. The question to be asked however, is "what the missile is programmed to do in such a case". The conventional missile is expected to store the last command and use it for control while first waiting, and later searching, for the lost target. Also, when the target has been reacquired, there is an initial period of pursuit navigation which is later switched to proportional navigation. All of the above described process can be handled by the adjoint method since switching at given times can be considered a time-varying gain (0 or 1).

Our purpose in this section is to find the relationships between the miss distance and the ECM and missile parameters. The questions of which missile parameters are observable, and how to derive ECM objectives will be discussed later.

The homing missile shown in Fig. 2.5 will now be augmented with a memory circuit designed to memorize a low-passed version of the last command; this is used to replace the regular command from the moment of break track to collision. Notice that collision in our terminology is the point in time and in space where the missile/target 3-D distance is minimum; because of the small disturbances assumed, this time is always given by $T_f = R_0/V_c$ of (2.3). It is also assumed that the ECM is designed to break track at an instant close enough to collision so that the search and reacquisition process cannot be completed. The last assumption allows us to omit the pursuit circuit and the corresponding switching between the two navigation laws.

Fig 4.1 shows the complete system to be analyzed in the sequel. The seeker's open-loop servo is realized with:

$$G = \frac{K(1+\tau_1 s)}{s(1+\tau_2 s)} \quad . \tag{4.1}$$

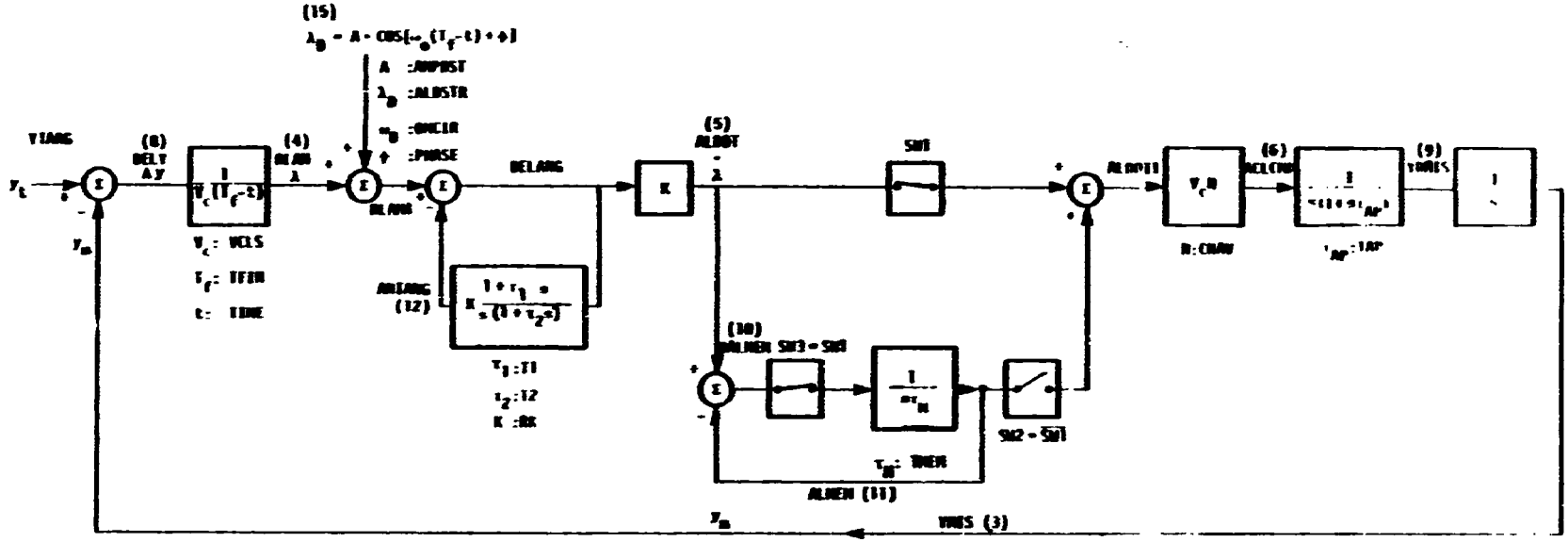

Figure 4.1 The Complete Homing Block Diagram

The closed loop seeker output is factored by the same open-loop gain, K, so that $\dot{\lambda}$ will have the units of rad/sec whenever λ is given in radians. The ECM effect is introduced through the additive line-of-sight disturbance λ_D . This disturbance can, in general, take any form; in Fig. 4.1 it is taken as the 1-D component of an ECM induced circular orbit, i.e.,

$$\lambda_D = A \cos [\omega_0(T_f-t)+\phi] \quad . \tag{4.2}$$

The disturbance phase with respect to collision can be chosen at will, and the amplitude, A = 0 or 1 , serves to introduce or delete λ_D in case other types of disturbances are of concern (such as λ_t).

The memory circuit is a simple first order filter which stores the filtered $\dot{\lambda}$; it sits in standby and has no effect (SW2 is open) as long as the seeker maintains a normal tracking. T_{sw} seconds before collision the track is broken and the memory circuit replaces the regular seeker output (SW1 = SW_3 are opened and SW2 closed). The memory circuit is built here so as not to discharge by opening (SW3) the input to the filter's integrator (Other methods, such as exponentially decaying memory, can also be used). The rest of the loop is the same as in Fig. 2.5 except that one of the geometrical integrations was included in the AP block (for use in the adjoint system).

The system of Fig. 4.1 can be directly transformed to yield its adjoint as shown in the closed-loop part of Fig. 4.2. This Figure should be compared with Fig. 3.3 to help identify the main functions. The leftmost integrator in Fig. 4.2 is one of the integrators imbedded in $W(\tau)$ of Fig. 3.3; it was separated from the rest of $W(\tau)$ so that an initial condition IC=1 can be assigned to it as a practical substitute for the Delta function shown in Figure 3.3. Notice that the transfer functions, or configurations containing only time-invariant components, are self-adjoint; for example, the seeker loop appears in Figure 4.2 in exactly the same form as it appears in Figure 4.1. Also, notice that the adjoint time, τ, runs from $\tau = 0$ at collision backwards so that the switches SW1 and SW3 are initially open while SW2 is initially closed.

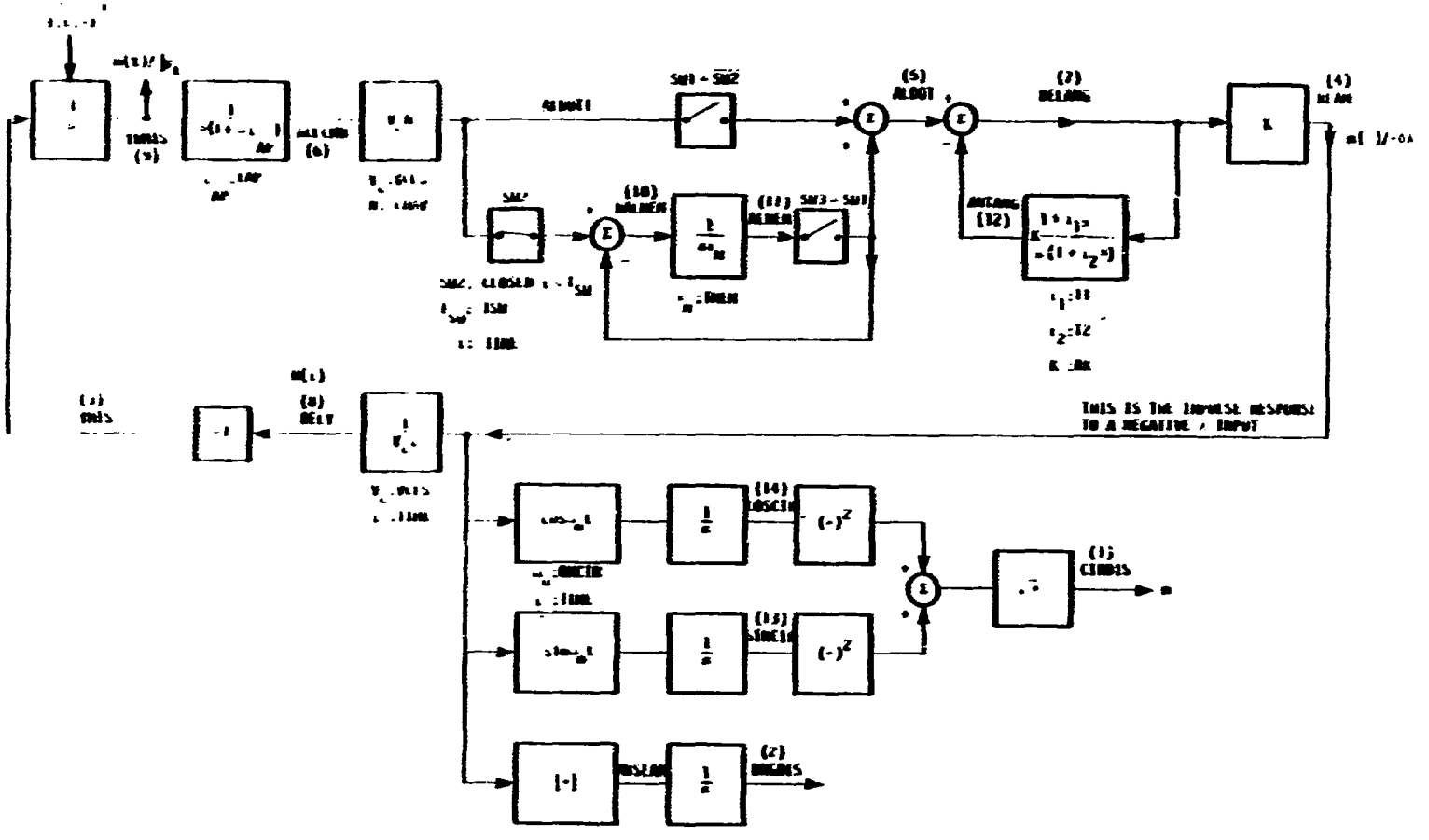

4.2 The Adjoint System Corresponding to the System of Figure 4.1

The output of the Adjoint System can, in general, be taken from any point to represent miss-distance responses to various types of inputs, disturbances or noise. In the case studied here only two responses are shown: $m(\tau)/\sqrt{Yt}$ (the response to a target displacement obtained at the output of the leftmost integrator) and $m(\tau)/\delta\lambda$ (obtained at the seeker's output at the right). The impulse response, $m(\tau)/\delta\lambda$, represents the miss-distance resulting from an impulse of disturbance in the line-of-sight angle λ (neglecting the minus sign). This basic output can now serve to derive responses to any type of λ disturbance through the use of the convolution technique.

Two types of ECM-induced λ-disturbances were studied, i.e., a (2-D) circular seeker orbit and a 1-D Bang-Bang optimal disturbance (or control from the viewpoint of the target). The idea of deriving a 2-D miss-distance response from the 1-D* (Pitch or Yaw) homing loop is explained by the following reasoning. A circular seeker orbit is composed of two 90° out-of-phase oscillations in the Pitch and the Yaw homing planes. The overall 2-D miss-distance must also be circularly symmetric since the Pitch and Yaw loops are assumed identical (in fact, because of symmetry considerations, the missile's trajectory in the 3-D space will be circular or spiral -- depending on the range). The above reasoning suggests that the miss-distance can be described by the phasor (in a plane perpendicular to the missile's velocity vector and containing the target) shown in Fig. 4.3. Notice that the Pitch axis in the Figure is the intersection of the Pitch plane (vertical to earth if the missile's roll is zero) and the Figure's plane; similarly, the Yaw axis is the intersection of the Yaw plane (not necessarily horizontal) and the Figure's plane. The phasor shown in Fig. 4.3 has a constant (although

---

* This should not be confused with the number of Degrees-of-Freedom (DOF). The 1-D situation refers to our planar treatment which may, in general, be performed with missile's equations written in 1, 2 or 3 DOF.

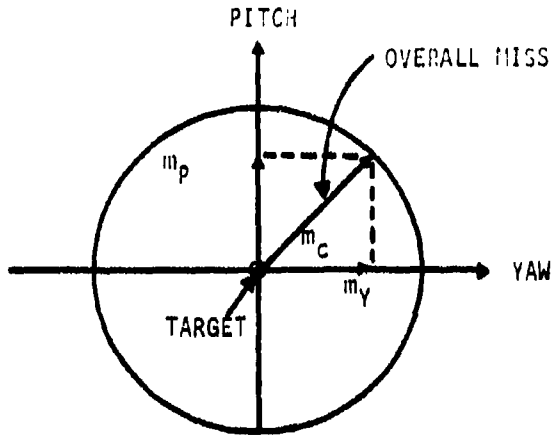

Figure 4.3 The Phasor Description of the Overall Miss-Distance

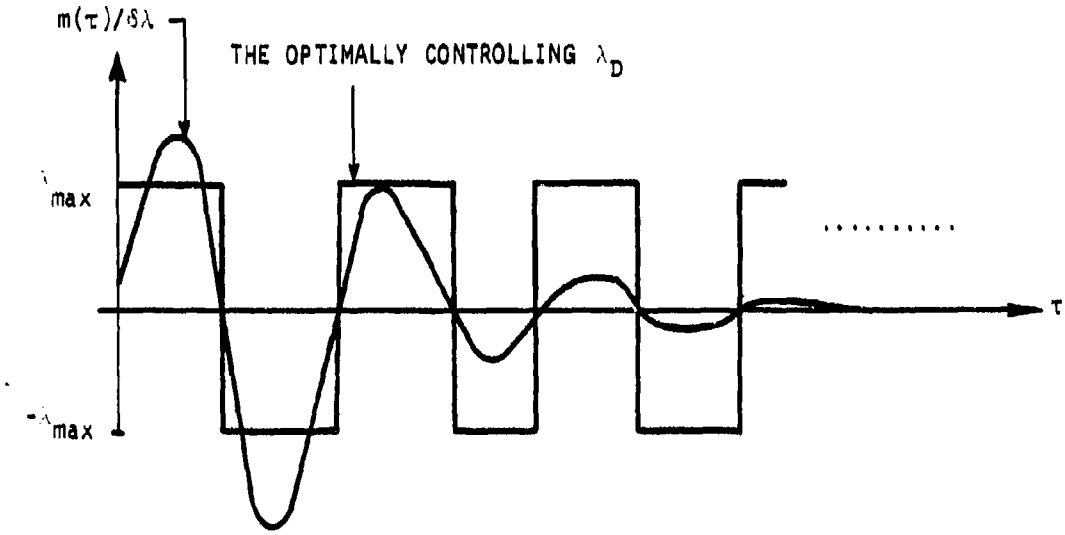

Figure 4.4 A Typical Miss-Distance Impulse-Response to a λ_D Input and the Corresponding Optimal Control

unknown) length and a phase which is determined by that of the seeker's orbit. Since only the length of the miss phasor is of concern, it can be obtained as:

$$m_c = \sqrt{m_p^2 + m_y^2} \quad , \tag{4.3}$$

where m_p and m_y are the Pitch and Yaw miss-distances obtained from two similar systems disturbed in parallel by (as in (4.2))

$$\lambda_p = \cos\ (\omega_0 t + \psi)$$

$$\lambda_y = \sin\ (\omega_0 t + \psi) \tag{4.4}$$

with any arbitrary disturbance phase ψ .

In practice, there is no need to run two Adjoint Systems in parallel to calculate m_p and m_y , and they can both be obtained from one run as shown in Fig. 4.2. Notice that factoring by, say, cos $\omega_0\tau$ and integrating in Fig. 4.2 is consistent with the input $\lambda_D = \cos\ [\omega_0(T_f - t)]$ in Fig. 4.1 ($\phi = 0$ since it makes no difference), since t should be replaced in the Adjoint System by $(T_f - \tau)$. Thus, convolving the 1-D miss-distance impulse-response with both the sin and the cos functions in parallel and taking the square-root of their squares results in the overall m_c of (4.3) as a function of the time-to-go τ .

The optimal-control ECM is evaluated in the following. The idea of optimally controlling the (1-D) miss-distance (which amounts to maximizing it) is explained with the help of Fig. 4.4 showing a typical miss-distance impulse-response. Assuming an amplitude-bounded controller, the optimal control is achieved by switching the control sign at the impulse-response zero-crossings (as shown in the Figure), i.e.:

$$\lambda_D = \lambda_{max}\ \text{SIGN}\ [m(t)/\delta\lambda] \quad . \tag{4.5}$$

The maximum effect obtained by using this control is

$$m_{max} = \lambda_{max} \int_0^{\infty} | m(\tau)/\delta\lambda | \, d\tau \quad . \tag{4.6}$$

The evaluation of m_{max} as above is performed by the bottom channal of Fig. 4.2.

5. NUMERICAL RESULTS

5.1 GENERAL

The block diagrams of Figs. 4.1 and 4.2 were coded into a comprehensive easy-to-use program. Table 5.1 gives a list of parameters which are used in the program and also appear in Figs. 4.1 and 4.2 (the Figures include the names of the program variables and the plot numbers (in parenthesis) as well.

The first step taken in using the simulation was to "design" a well behaved missile. The main design parameters in the configuration of Fig. 4.1 are:

$$N,\ \tau_{AP},\ K,\ \tau_1,\ \tau_2 \ .$$

A navigation constant of $N = 3$ was chosen to enable the missile to achieve a converging (to zero) miss against a constant accelerating target as explained in Section 3 (see Eq. (3.7)). The closed-loop AP time-constant, τ_{AP}, was taken as 0.5 sec to represent a well-designed AP of a reasonably sized, say 200 kg, missile. The three antenna parameters were, at first, chosen to correspond to the APQ-112 which caused the homing loop to diverge. Realizing that this antenna was not designed for a homing missile, it was later replaced with the Triple-S antenna (with compensation) which was originally designed for the Harpoon missile. This antenna, which is represented by:

$$K = 126\ ;\ \tau_1 = 0.03\ ;\ \tau_2 = 0.3\ ,$$

yielded excellent results (for the missile) as judged from the behavior of the miss impulse-response (damping rate and area).

The closing speed, V_c, can vary vastly between $V_m + V_t$ (in a head-on course) and $V_m - V_t$ (assuming $V_m > V_t$). For example, if V_m=600 m/sec and $V_t = 300$ m/sec, $300 \text{ m/sec} < V_c < 900$ m/sec. A medium speed of 600 m/sec was arbitrarily chosen to work with. Examining Fig. 4.2, it is noticed that V_c cancels out in the main loop, so that $m(\tau)/\_|\overline{Y_t}$ is

Table 5.1 Parameters Used in the Program

PARAMETER SYMBOL	PROGRAM SYMBOL	USED IN
τ_{AP}	TAP	Auto-pilot time constant
N	CNAV	Proportional navigation gain
V_c	VCLS	Missile/target closing speed
ϕ	PHASE	Phase of the circular seeker orbit
T_{SW}	TSW	Break-track time before collision
τ_M	TMEM	Memory circuit time constant
k	RK	Seeker open-loop gain
τ_1	T1	Seeker zero time-constant
τ_2	T2	Seeker pole time-constant
ω_o	OMCIR	Orbit radian frequency
T_f	TFIN	Run time of simulation
-	SAMRAT	Integration steps per second
-	IFWBW	Original/adjoint switch: 1 - original; 2 - adjoint

independent of it. However, $m(\tau)/\delta\lambda$ is linearly dependent on V_c, since it is tapped from a point already factored by V_c (the block V_cN). Thus, all the miss results derived from $m(\tau)/\delta\lambda$ can be later adjusted (or normalized) to any desired V_c.

The memory parameter, τ_M, is in general not simple to choose since it should be optimized for the expected noise, glint, expected target maneuvers, etc. A typical $\tau_M = 0.5$ sec was chosen quite arbitrarily.

The second step, after having defined the missile and scenario, was to compare the results of the Forward (original system) and Backward (adjoint system) runs. Figure 5.1 is an adjoint run which shows $m(\tau)/\sqrt{Y_t}$. Figures 5.1a - d show forward runs corresponding to points A - D in Fig. 5.1. It can be checked that the values of Δy at collision agree with those read from Fig. 5.1. Figures 5.2 and 5.2a - d make a similar comparison for the case where break track (BT) occurs 1 sec before collision, i.e. $T_{SW} = 1$ sec . Comparing Figs. 5.1 and 5.2, it is noticed that the miss in Fig. 5.2 can go much higher than the original 1 m displacement ($\sqrt{Y_t}$) , whereas Fig. 5.1 shows a well-behaved damped response. The reason for the first negative peak in Fig. 5.2 is that, at first, the missile makes a vigorous correction which results in a large overshoot since BT occurs about 0.1 sec after homing has been initiated. Also, it is noticed that the memory circuit behaves excellently, since Fig. 5.2 shows an asymptotic approach to zero (which can also be seen from the small miss of Fig. 5.2d.

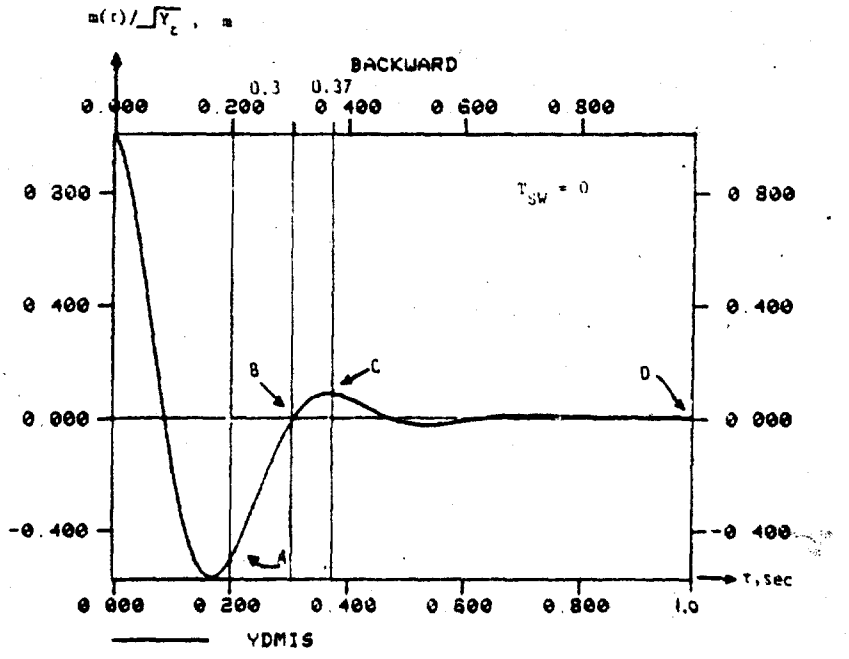

Figure 5.1: An adjoint run showing $m(\tau)/\sqrt{Y_t}$. Points A, B, C, D are compared with forward runs in Figures 5.1a through 5.1d.

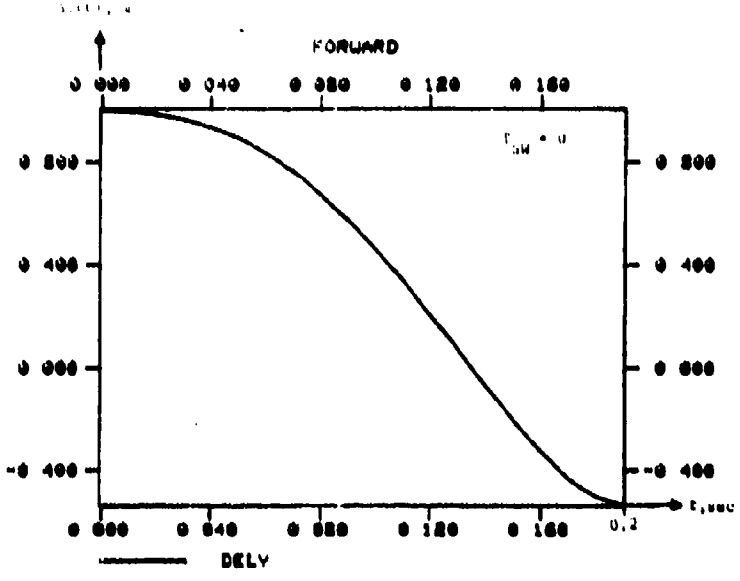

Figure 5.1a: Miss for a 0.2 sec forward run.

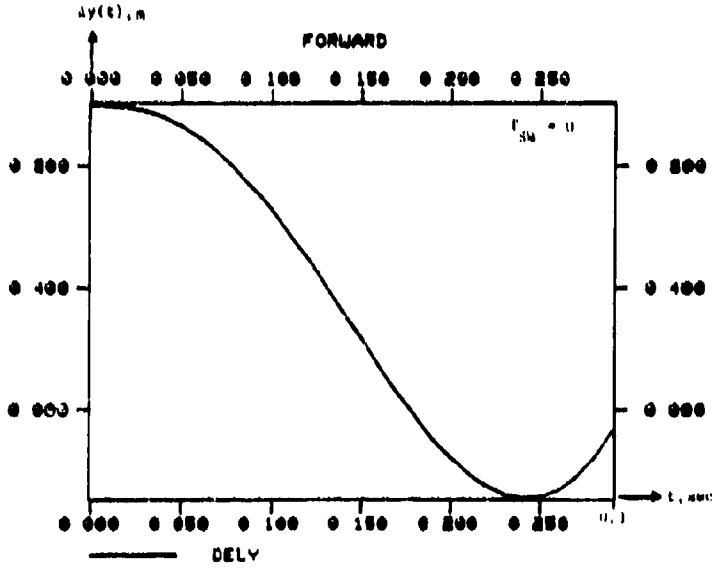

Figure 5.1b: Miss for a 0.3 sec forward run.

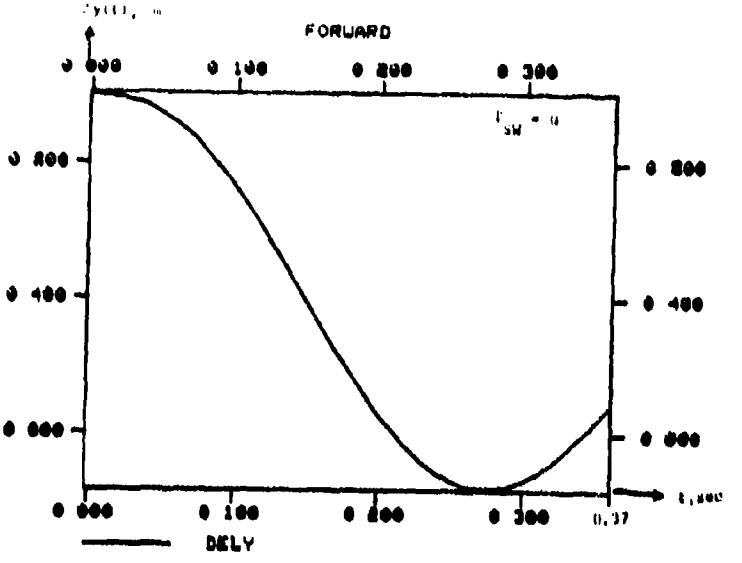

Figure 5.1c: Miss for a 0.37 sec forward run.

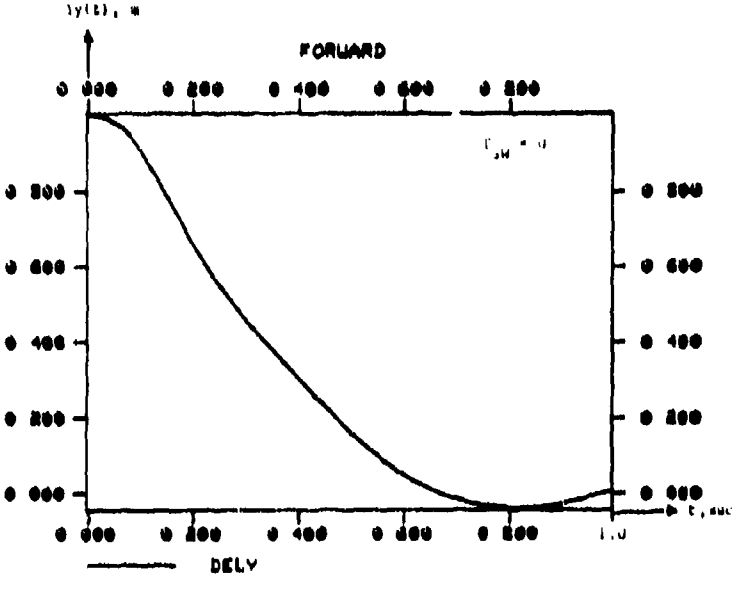

Figure 5.1d: Miss for a 1.0 sec forward run.

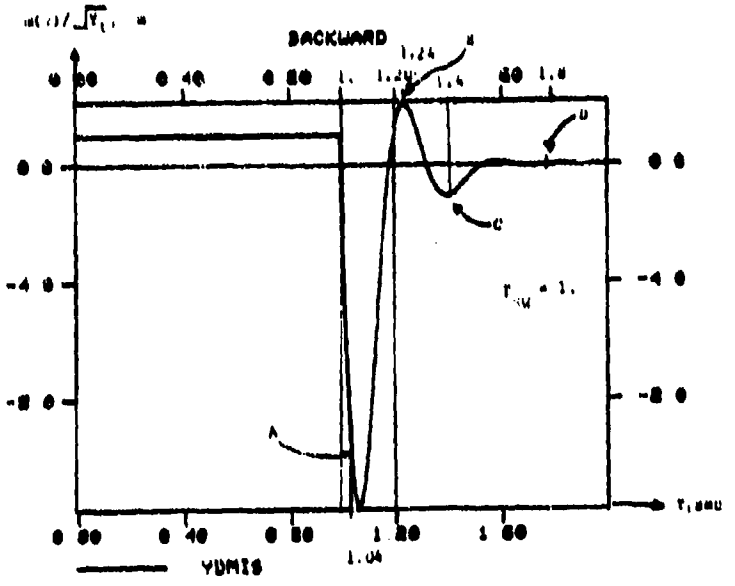

Figure 5.2: An adjoint run showing $m(\tau)/\sqrt{Y_t}$ for $T_{sw} = 1$ second. Points A, B, C, D are compared with forward runs in Figures 5.2a through 5.2d.

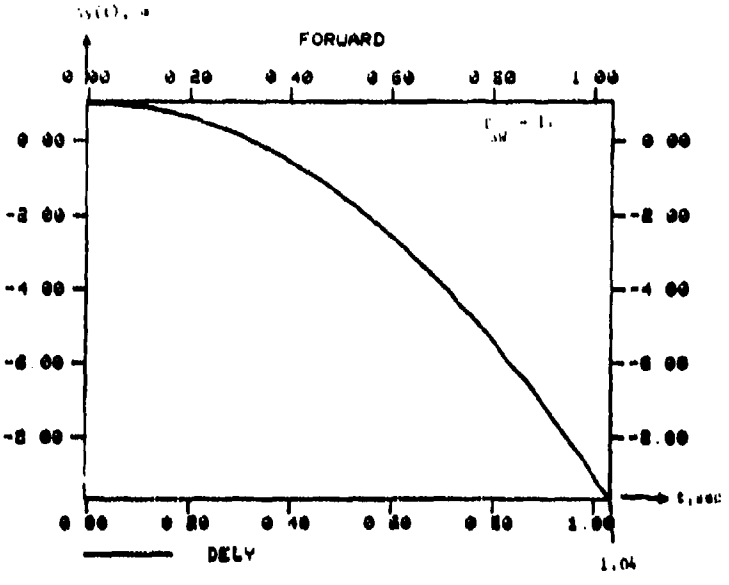

Figure 5.2a: Miss for a 1.04 sec forward run.

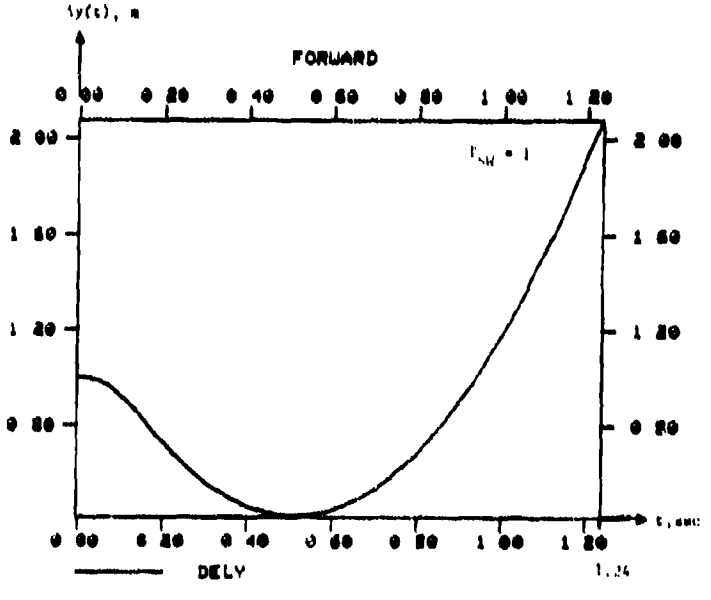

Figure 5.2b: Miss for a 1.24 sec forward run.

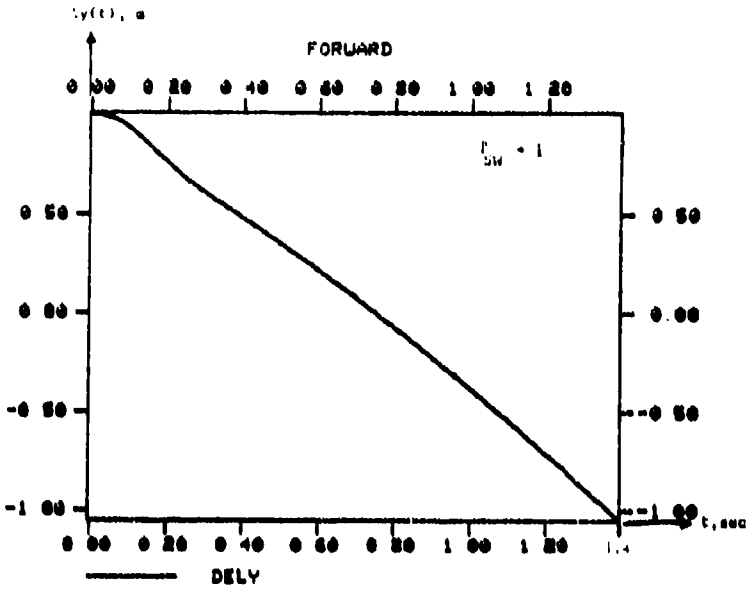

Figure 5.2c: Miss for a 1.4 sec forward run.

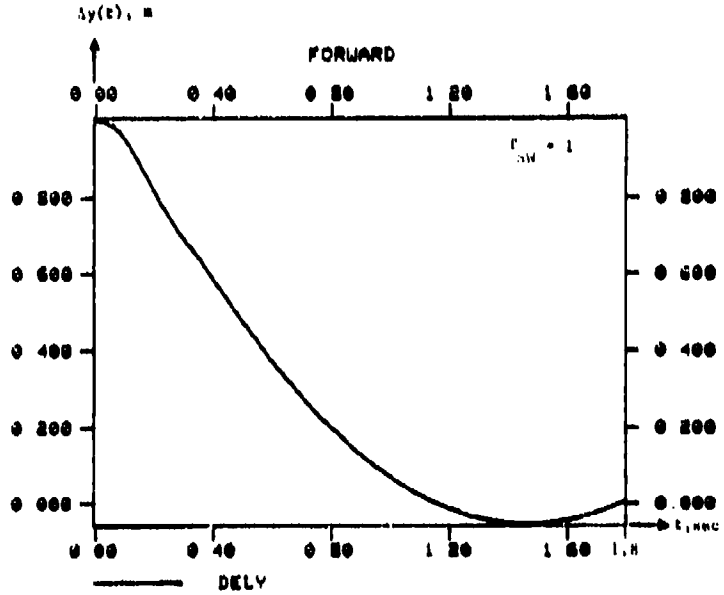

Figure 5.2d: Miss for a 1.8 sec forward run.

5.2 MISS-DISTANCE RESPONSES WITH NO BREAK-TRACK

The following material presents the miss-distance results which are relevant to the case of ECM-induced circular disturbance λ_D. The impulse response, $m(\tau)/\delta\lambda$, itself is the basic result from which all the others are derived; although it has no direct use, it serves to convey some very useful information such as the homing-loop natural frequency, damping rate, gain, and time extent.

Figure 5.3 shows the miss-distance impulse response to a λ_D input. Notice that all miss figures are normalized to a unity λ-input; for example, a 1-radian area λ-impulse applied 0.1 seconds before collision would cause a 800 meters miss (point A in the figure). On the other hand, if the same input is applied more than a second before collision, it would cause a negligible miss as is obvious from the figure. The meaning of the above observation is that any type of λ disturbance applied more than a second before collision is ineffective. The homing-loop "natural frequency" is another important characteristic obtained from the impulse-response behavior; its value of about $\omega_0 = 19$ rad/sec serves for the circular orbit disturbances shown in Figs. 5.4 to 5.6.

Figure 5.4 shows the miss response to a $\cos(\omega_0 t)$ input (having a 1-rad amplitude). Three corresponding forward runs are shown in Figs. 5.4a - c; it is noticed that for $t > 1$ sec all miss distances are equal (70 m) as predicted from the asymptotic approach of the adjoint graph to -70 m in Fig. 5.4 (all backward λ results are shown reversed in polarity). Figure 5.5 shows the response to a $\sin(\omega_0 t)$ input (which happens to approach a larger final value of 150 m), and Fig. 5.6 shows the combined 2-D circular miss response.

The optimal control (OC) response is given in Fig. 5.7 and yields a maximum miss of 225 m for control bounded by $\pm$ 1 rad. Comparing this final value with the circular miss final value of 170 m suggests that the circular disturbance (at the above frequency) is quite an effective ECM method.

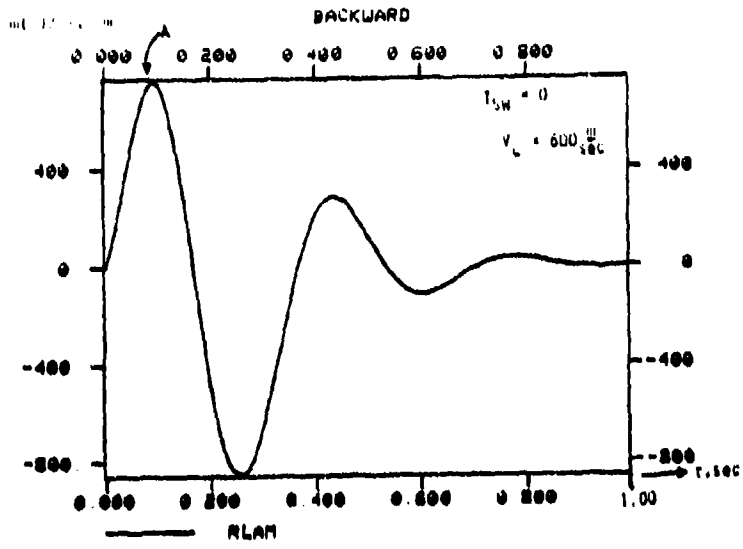

Figure 5.3: The miss-distance impulse-response.

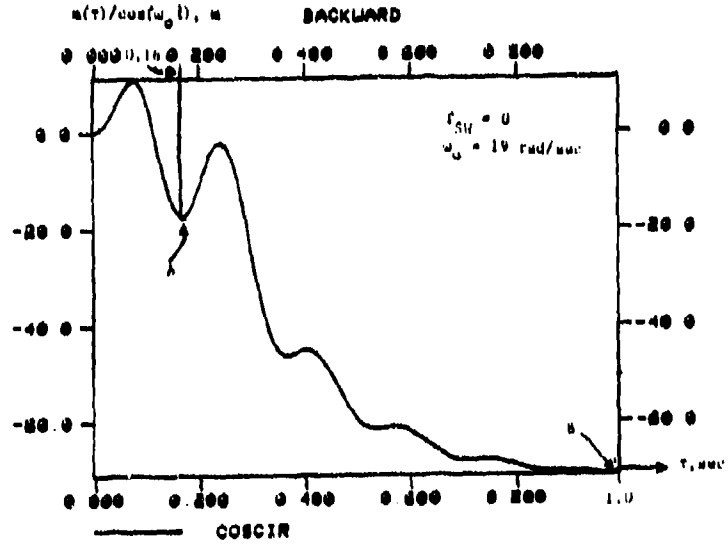

Figure 5.4: Miss-distance given a $\cos(\omega_0 t)$ disturbance.

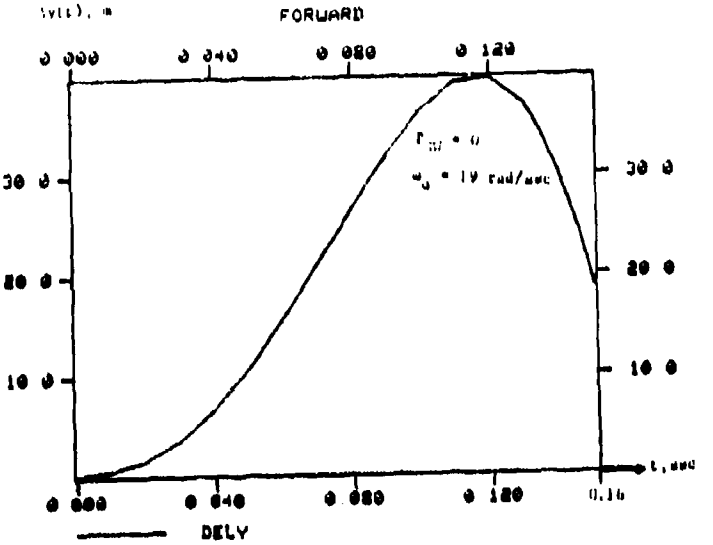

Figure 5.4a: A 0.16 sec forward run with a $\cos(\omega_o t)$ disturbance (see point A in Figure 5.4).

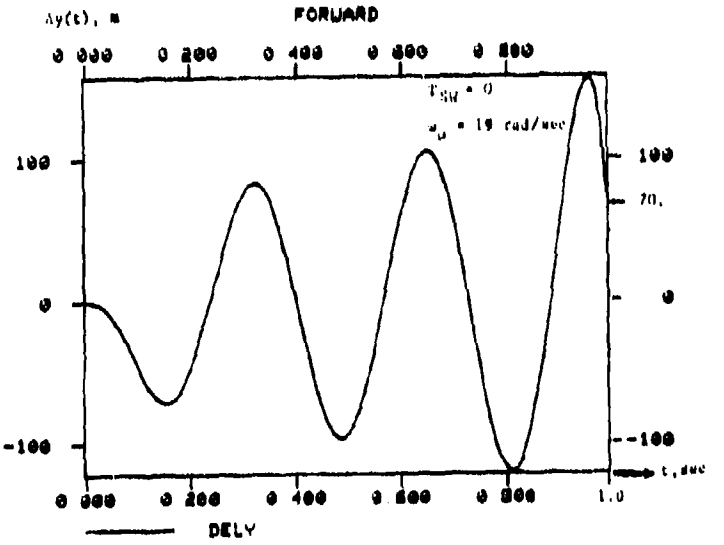

Figure 5.4b: A 1 sec forward run with a $\cos(\omega_o t)$ disturbance (see point B in Figure 5.4).

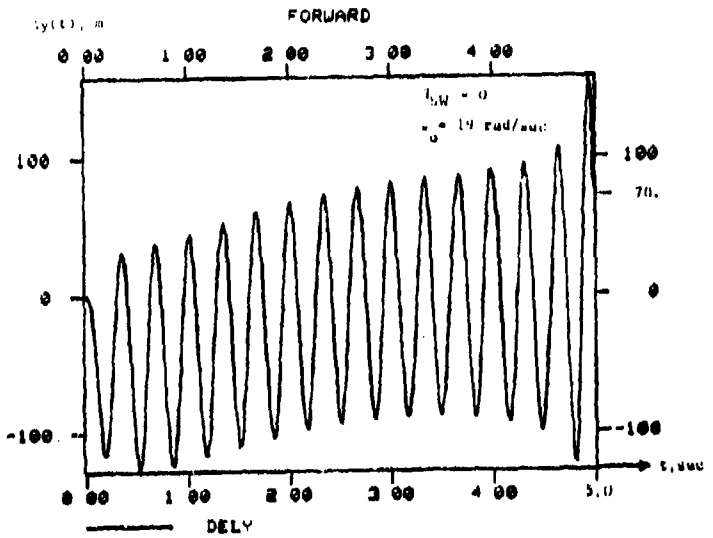

Figure 5.4c: A 5 sec. forward run with a cos ($\omega_0 t$) disturbance.

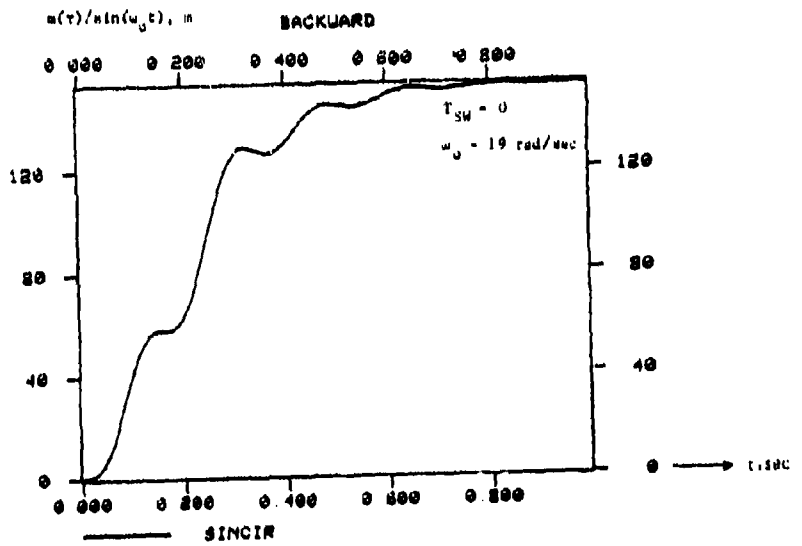

Figure 5.5: Miss-distance given a sin($\omega_0 t$) disturbance.

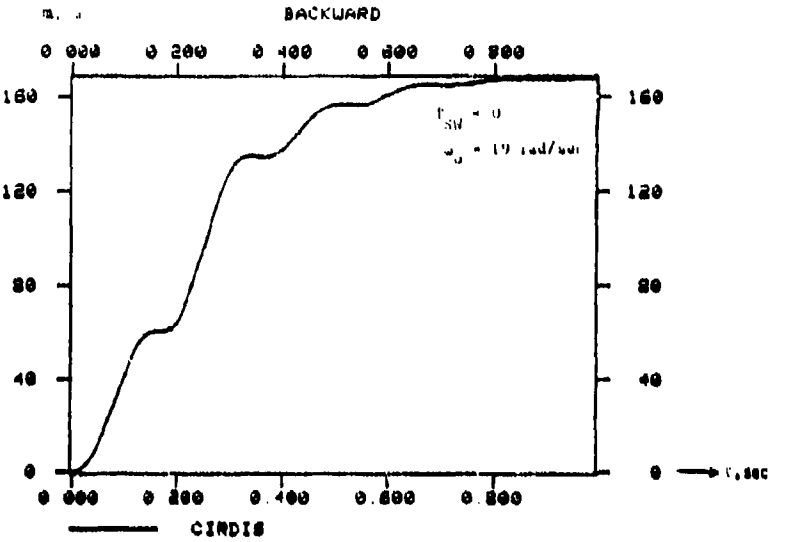

Figure 5.6: The 2-D circular miss response.

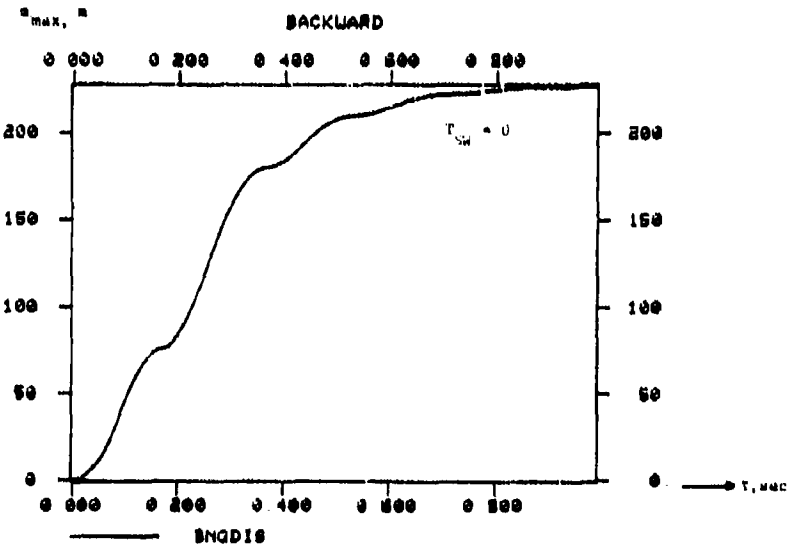

Figure 5.7: The optimal-control miss response.

5.3 THE EFFECT OF BREAK-TRACK ON THE MISS DISTANCE

The effect of an early Break-Track (BT) is investigated in the next series of figures (5.8 to 5.11) and summarized in Fig. 5.12. Figures 5.3, 5.8, 5.9, and 5.10 show the behavior of the $m(\tau)/\delta\lambda$ impulse responses as the BT time increases from 0 to 0.1, 0.5, and 1 secs, respectively. It is observed that, aside from the sharp peak immediately adjacent to the BT instant (as explained in conjunction with Fig. 5.2), the response is basically similar in shape (natural frequency and time extant); it is, however, shifted by T_{sw} to the right and enormously amplified. Also, it should be indicated that all impulse responses go to zero at large homing times-- meaning that disturbances applied a long time before collision have negligible effect even with an early BT.

Figures 5.7, 5.8a, 5.9a, 5.10a, and 5.11 show the optimal-control miss. It is observed that these graphs are also shifted by T_{SW} and amplified monotonically with T_{SW}. Figure 5.12 summarizes the asymptotic values of the optimal control miss as a function of the BT time (the m_B graph will be used later). It is clear that the payoff involved with an early BT is very high-- up to 3 orders of magnitude for 3 sec of T_{SW}.

The sensitivity of the circular orbit miss, m_C, to the orbital frequency, ω_0, is shown in Fig. 5.13. This result will be discussed in Section 6.2.

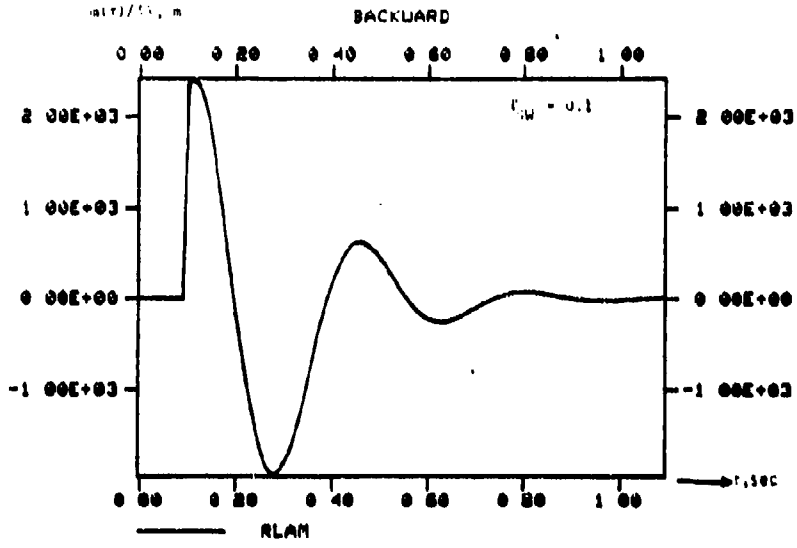

Figure 5.8: The miss-distance impulse-response with break-track 0.1 sec before collision

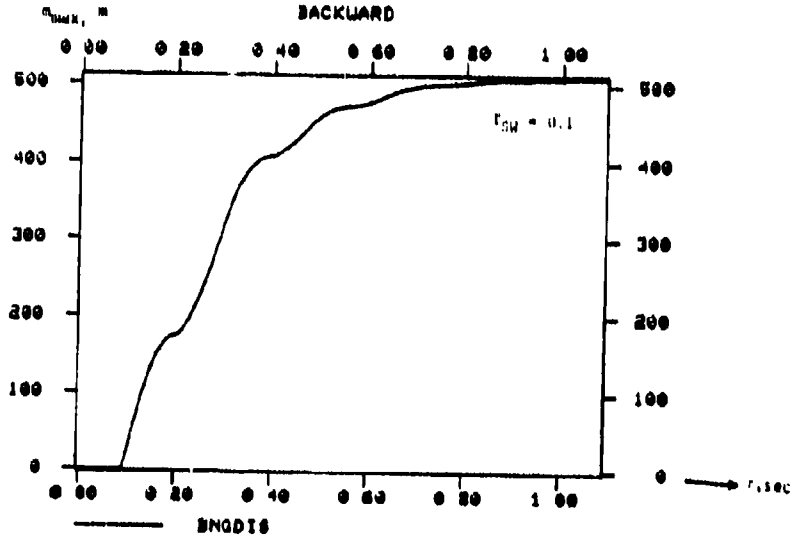

Figure 5.8a: The optimal-control miss-response with T_{SW} = 0.1

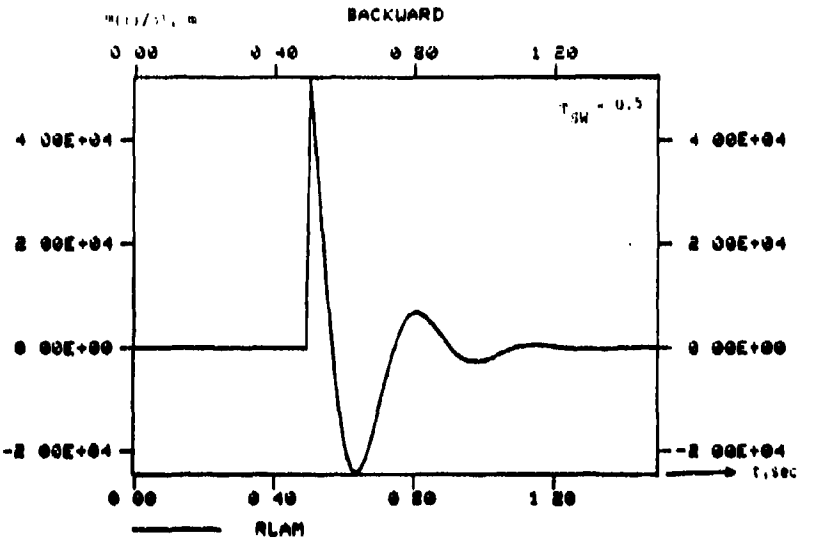

Figure 5.9: The miss-distance impulse-response with $T_{SW} = 0.5$

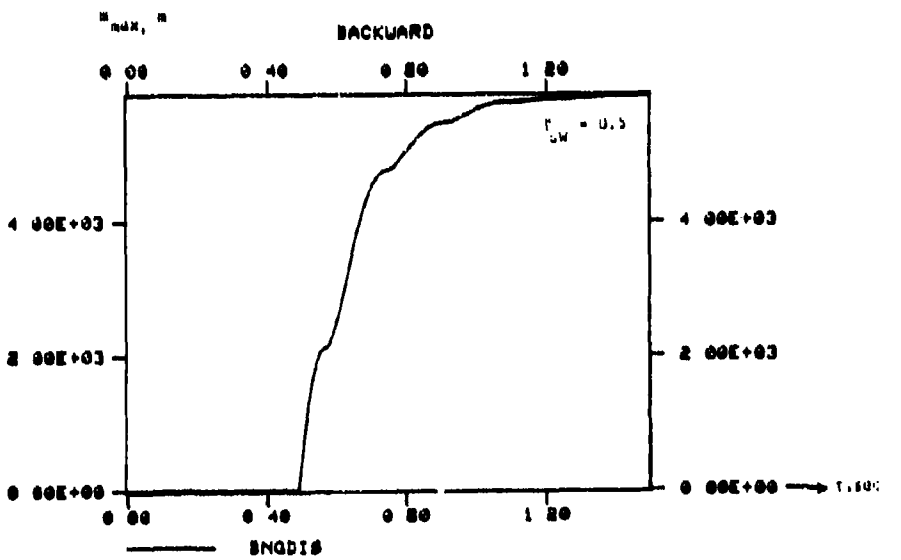

Figure 5.9a: The optimal-control miss-response with $T_{SW} = 0.5$

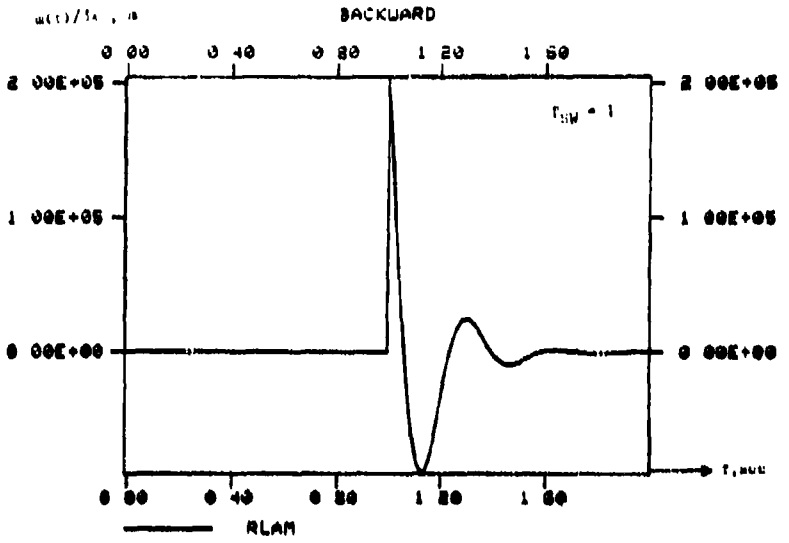

Figure 5.10: The miss-distance impulse-response with $T_{SW} = 1$

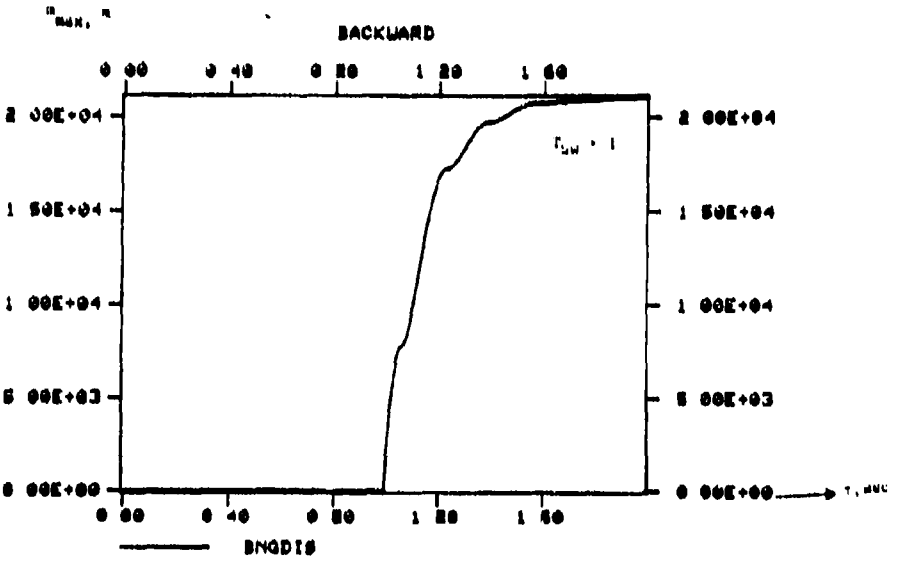

Figure 5.10a: The optimal-control miss-response with $T_{SW} = 1$

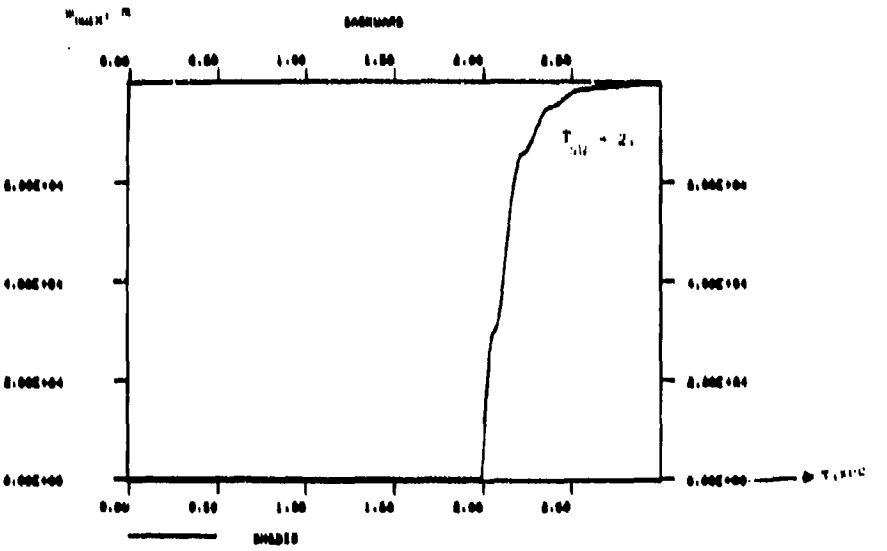

Figure 5.11: The optimal-control miss-response with $T_{SW} = 2$.

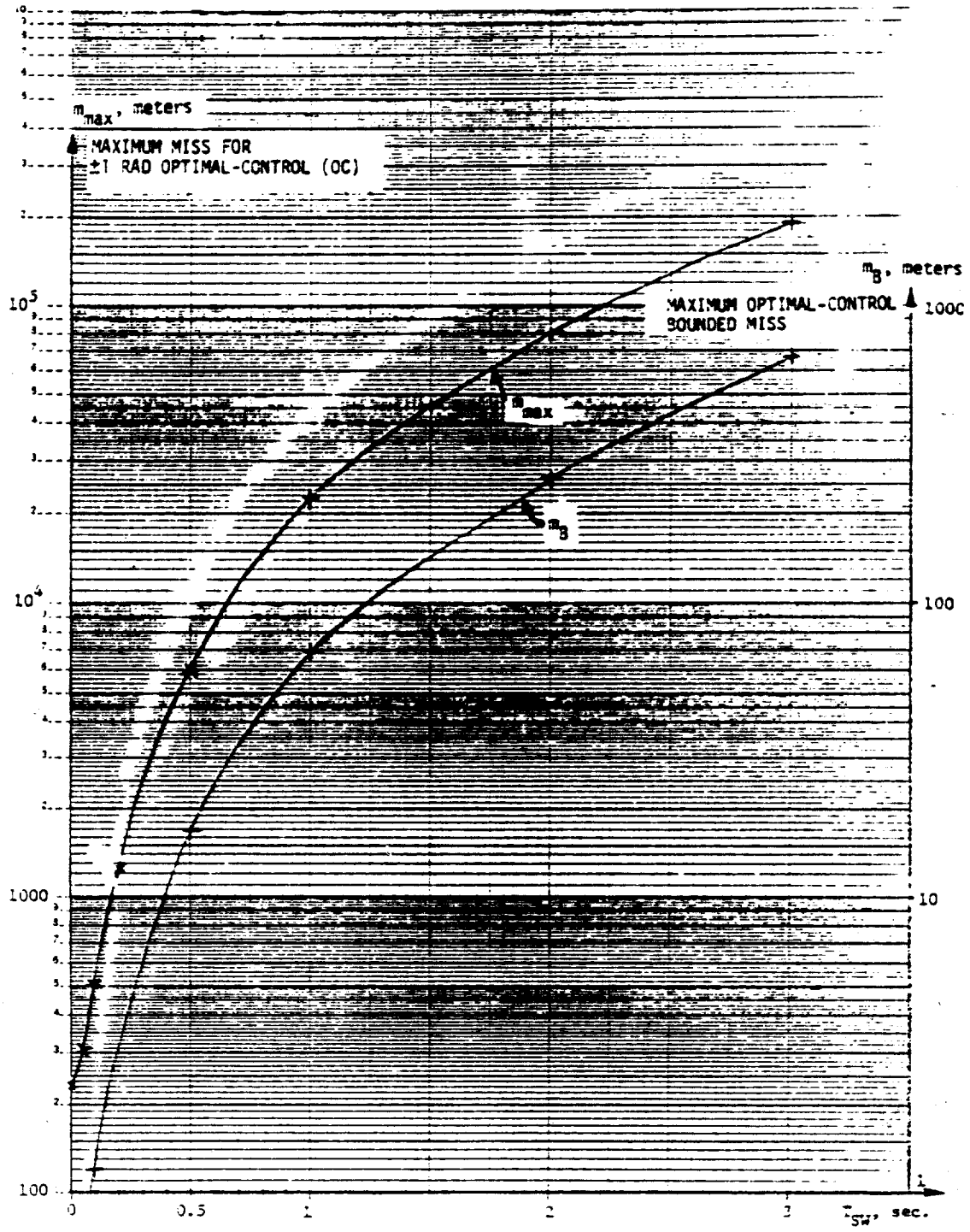

Figure 5.12: The asymptotic values of the ± 1 radian Optimal-Control miss and the bounded Optimal-Control miss as a function of the early Break-Track time, T_{sw}.

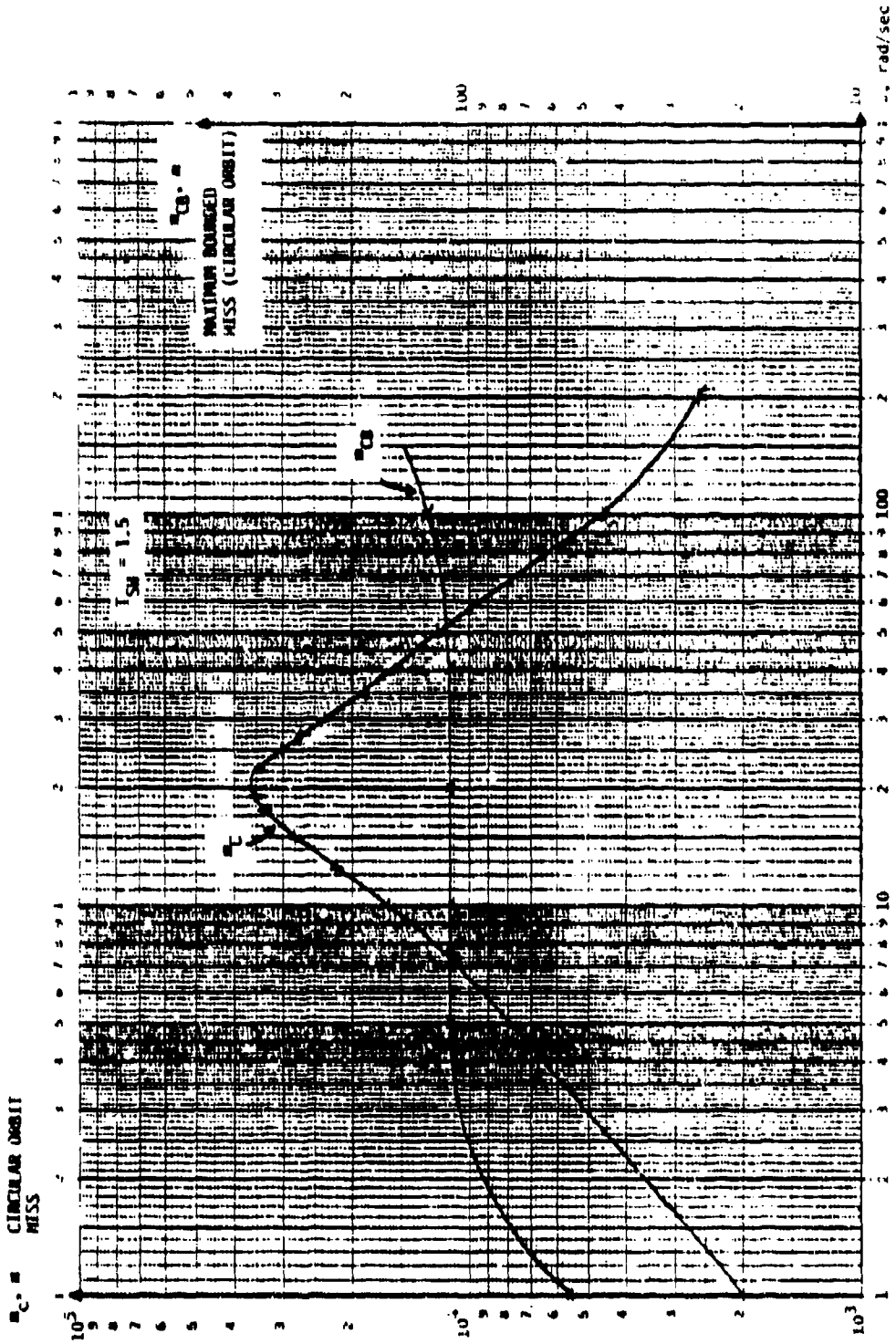

Figure 5.13: The dependence of the circular orbit mass on the orbital frequency.

5.4 NON-LINEAR EFFECTS ON THE ACHIEVABLE MISS DISTANCE

Up to this point the homing loop has been considered as a time-varying linear system. However, in practice there are some bounded variables within the loop that limit the validity of the above results to only those cases complying with the bounds. Although bounds exist on all missile entities, only one or two variables actually tend to hit their limits; these are usually the seeker error and the acceleration command to the AP (DELANG or ε and ACLCMD or a_C in Fig. 4.1).

The actual acceleration command values are usually much smaller than those obtained in our forward runs since, in many cases, a_c is first filtered (to attenuate the seeker's noise) and only then bounded. Graphs of the memory filter output (ALMEM or a_{CM}) are thus included to show the effect of such a filter on the a_C amplitude. Although a typical noise filter may have a time-constant of about 0.1 - 0.2 sec , the 0.5 sec memory filter used here can still serve to indicate the tendency of considerably attenuating a_C.

The method adopted here is the following. Optimal-control forward-runs results should be scaled down so as to contain them within their respective bounds for all times. The most limiting scaling factor should then be used to scale the misses read from the OC backward runs. Since it is much simpler to deal with circular orbit (CO) forward runs than with OC forward runs, the CO forward runs were used to obtain the scaling factor which was then applied to the backward OC runs. This practical procedure is based on the assumption that about the same factor will apply to both OC and CO results.

Consider, for example, the figure set 5.14, where $T_{SW} = 0.5$ and:

$$\varepsilon_{max} = 1.45 \text{ rad} \; ; \; a_{C_{max}} = 3.3 \cdot 10^5 \text{ m/sec}^2 \; ; \; a_{CM_{max}} = 3.6 \cdot 10^4 \text{ m/sec}^2.$$

Assuming bounds of 1.5° (or 26 mrad) on ε , 15 g (or 150 m/sec^2) on a_C and 10 g on a_{CM} requires scaling by:

$1.8 \cdot 10^{-2}$ for ε ; $4.5 \cdot 10^{-4}$ for a_C and $2.8 \cdot 10^{-3}$ for the filtered command .

It is obvious that the ε bound poses no problem and that a_C is the most limiting paramater. We will, however, use the a_{CM} factor because of the above comment (regarding the missing noise filter) and because a_{CM} , in this case (where $\tau_M = \tau_{AP}$) , also represents the actual missile's acceleration. Thus, only the a_{CM} factor will be used in the sequel. Reading the maximum miss from Fig. 5.12 for $T_{SW} = 0.5$ and factoring yields:

$$m_B(T_{SW} = 0.5) = 6000 \cdot 2.8 \cdot 10^{-3} = 16.8 \text{ m} ,$$

where m_B denotes the bounded OC maximum miss. Repeating the above procedure for other T_{SW} values yields the following results:

TABLE 5.2: The Bounded Misses

T_{SW}, sec	0.1	0.5	1	2	3
a_{CM}, m/sec^2	$4.2 \cdot 10^4$	$3.6 \cdot 10^4$	$3.2 \cdot 10^4$	$3.1 \cdot 10^4$	$2.9 \cdot 10^4$
a_{CM} factor	$2.4 \cdot 10^{-3}$	$2.8 \cdot 10^{-3}$	$3.1 \cdot 10^{-3}$	$3.3 \cdot 10^{-3}$	$3.5 \cdot 10^{-3}$
m_B, meters	1.2	16.8	69	260	665

The m_B results are also shown in Fig. 5.12.

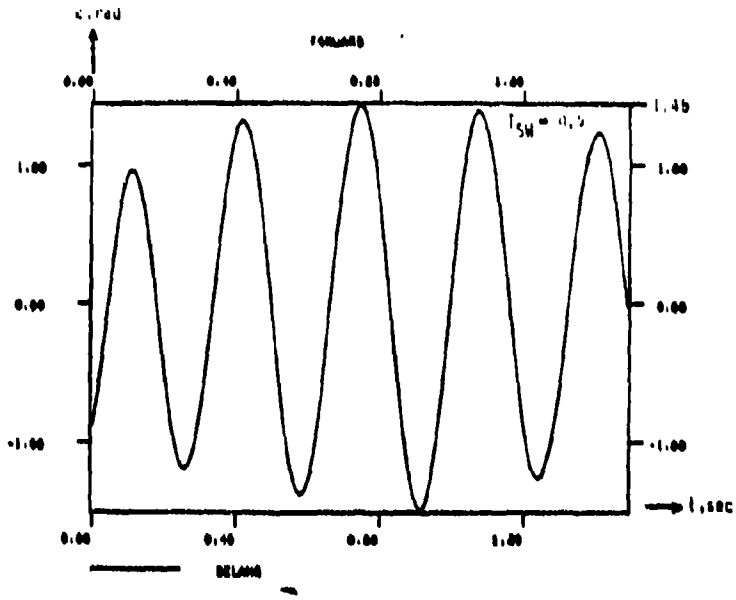

Figure 5.14: Seeker's error for a 1-rad amplitude circular disturbance.

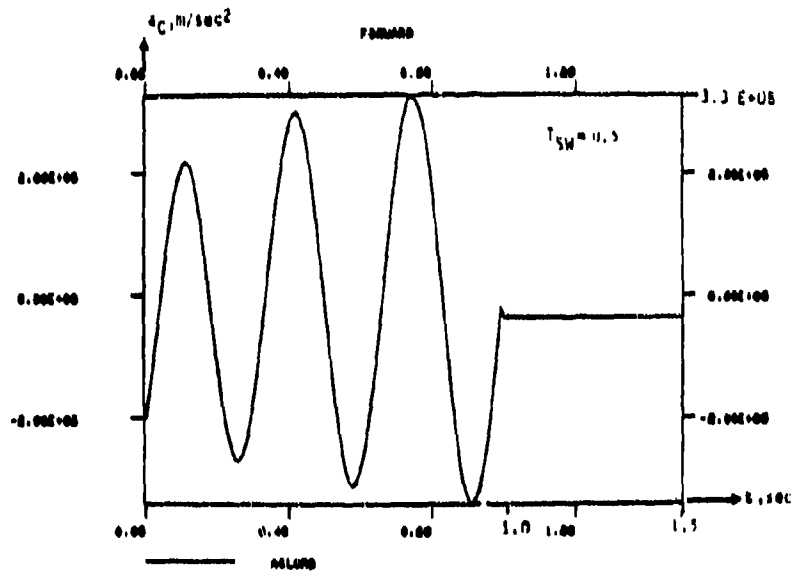

Figure 5.14a: Acceleration command for a 1-rad amplitude circular disturbance.

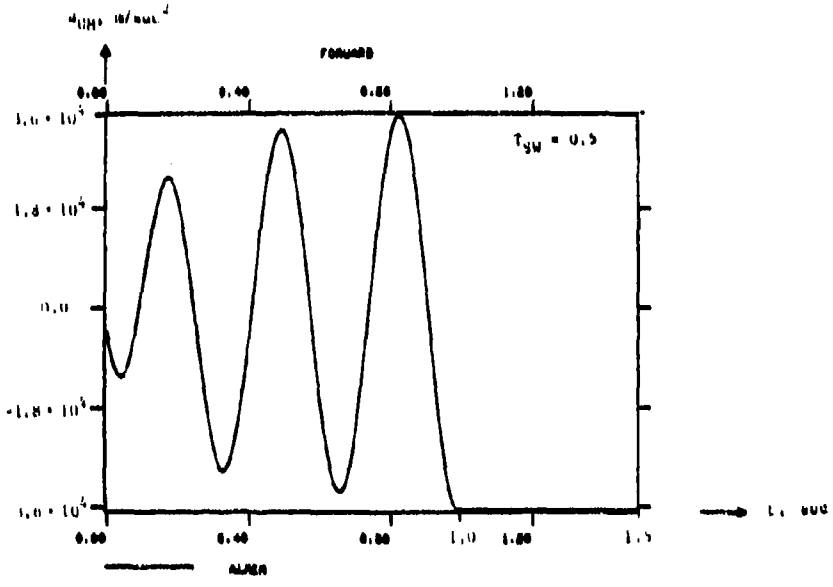

Figure 5.14b: Filtered (τ_w = 0.5 sec) acceleration command for a 1-rad amplitude circular disturbance.

6. THE REQUIRED OBSERVABLES (OR PRIOR KNOWLEDGE)

The potential of inducing a very large miss-distance through the employment of an appropriate ECM has been discussed in the previous sections. The actual harnessing of this potential to the benefit of the ECM carrying target depends on its available observables. Let us now discuss the question of which observables (and at what accuracy) are required for the main two ECM methods, namely the circular orbit and the optimal control.

6.1 THE OPTIMAL CONTROL OBSERVABLES

The optimal-control (OC) ECM is the most demanding, in terms of observables, because it has to figure out the zero-crossing points of the appropriate backward run in real time. Ideally, the target should at least have the level of knowledge required to construct the adjoint (or forward) system as shown in Fig. 4.2. Since it is very unlikely for the target to search for parameters, such as τ_{AP} , τ_M , τ_1 , τ_2 , N, etc., (see Table 5.1) during the actual engagement, it seems that only a priori detailed knowledge of the attacking missile can enable the use of the optimal control ECM. Further work is required to study the information content of the unexcited missile's oscillations.

The above conclusion does not exclude the use of the OC method, since one can envisage programming an ECM computer according to Fig. 4.2 and feeding it with various missile's parameter sets as they are obtained from intelligence sources. In such a scenario the only real-time identification that has to take place is with respect to the attacking missile type. This can be made on the basis of real-time radar measurements such as RF carrier, PRF, pulse-width, or a complete pulse footprint analysis. There are still two more engagement (not missile) parameters that have to be figured out in real-time; these are the initial range, R_0 , and the closing speed, V_c .

The OC method can be used in either a 1-D or 2-D mode. The 2-D overall miss will be a factor of $\sqrt{2}$ higher than the 1-D miss.

6.2 THE CIRCULAR-ORBIT OBSERVABLES

The circular-orbit (CO) ECM method is much simpler than the OC method in terms of observables, since it deals with the overall 2-D miss and not with the 1-D optimally controlled miss. This 2-D versus 1-D difference is crucial since no phase, or exact synchronization with respect to the collision instant, is required. The main parameter to be chosen is the orbital frequency, and it turns out that the miss-distance is quite insensitive to that frequency also. Figure 5.13 shows a miss peak at $\omega_0 = 20$ rad/sec which is the peak frequency of the closed-loop seeker as shown in Fig. 6.1. This is not surprising since the homing loop can be considered open-loop for large ranges ($1/R(t)$ appears in the feedback path for the disturbance λ_D in Fig. 4.2), and the only components appearing in the forward path are the closed loop seeker and the AP time-constant (at a much lower frequency). Since the interesting cases are those where BT occurs at around 1 - 3 seconds , the $1/R(t)$ factor is always large and has only a small effect during the active homing period (before BT).

Although Fig. 5.13 (for a constant $T_{SW} = 1.5$ sec) shows a peak in the CO miss, it does not show any in the bounded CO miss, m_{CB} (obtained as in Section 5.4). The reason for the almost constant m_{CB} is that the actual limiting point is at the AP input so that a larger ECM disturbance can be applied to compensate for the seeker attenuation at frequencies far from the peak without causing ε limiting.

The conclusion regarding ω_0 is that almost any frequency used for the disturbance, having amplitude within the seeker's linear region, can induce misses of around 75% of those given by the 1-D m_B graph of Fig. 5.12 as a function of the BT time T_{SW}.

The second parameter to be chosen is the BT instant. Two kinds of inputs are required for this purpose, i.e. the time-to-go and TSW. The time-to-go can be calculated on the basis of range $R(t)$ and range-rate (V_c) estimates obtained from the received power. A much

simpler data source may be an on-board probing radar which can measure $R(t)$ and V_c directly. The T_{SW} parameter can be either obtained from intelligence as the average time of reacquisition or can be "probed" in real-time. Probing for T_{SW} can be performed by breaking track early in the engagement and measuring the actual reacquisition time.

An entirely different approach to defeat the missile can be conceived in cases where one knows some more specifics about it. Most missiles use a pneumatic or hydraulic power source to drive the seeker and the deflection surfaces. This power source is quite limited and in many cases determines the far end of the missile's "fire zone". The circular ECM disturbance can drain this source much faster than expected and effectively contract the actual fire-zone. Thus, a missile which was fired at a target at, say, the farther half of its fire-zone, may run out of power in mid way causing a substantial "miss-distance".

The only ECM consideration in such a case is to cause the highest power drain possible (which is, usually, proportional to ω_Q for a given amplitude). In addition to that, the target has to estimate the launching range and to have a good idea about the fire-zone shape.

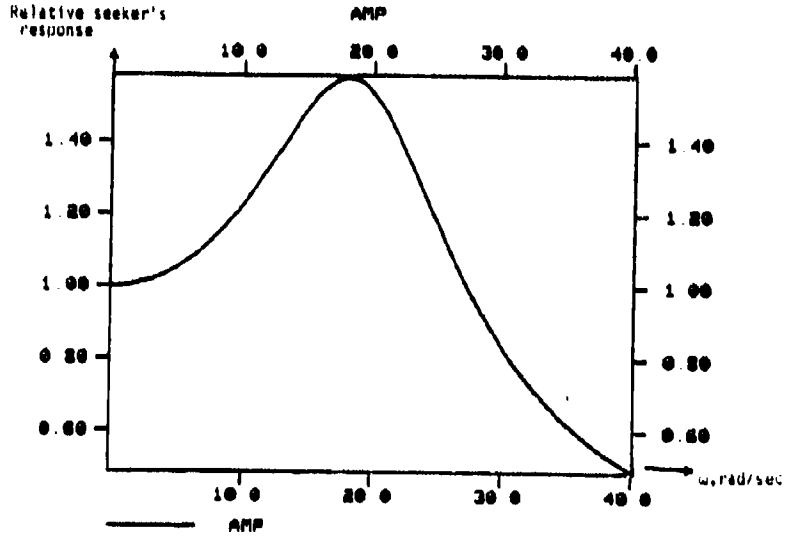

Figure 6.1: The seeker's closed-loop response

7. OPERATIONAL SUMMARY

7.1 CIRCULAR ORBIT ECM

- T_{SW} obtained from either:
  - intelligence sources
  - probing by causing an early BT.
- ω_0 obtained from either:
  - intelligence
  - searched for in real time to cause an antenna orbit of about 1° radius.
- Time-to-go (R(t) and V_c) from either:
  - probing radar
  - estimated on the basis of received power.

7.2 FIRE-ZONE "MODIFICATION" THROUGH A CIRCULAR ECM

- Maximum fire-zone range from:
  - intelligence
- Launch range
  - estimated based on the received power, aircraft altitude, etc.
- ω_0 from:
  - a real-time search for the highest frequency at which the antenna can be caused to orbit at, say, 1° radius.
- Fire-zone contraction factor as a function of ω_0:
  - intelligence

8. CONCLUSIONS AND FUTURE WORK

The ultimate objective of a closed-loop ECM has been identified as the maximization of the miss-distance. This objective can be pursued in many ways, among which is the induction of a circular orbit to the missile's seeker; this orbit is known to be achievable in the cases of conical-scan and SWIC radars.

The real-time observables, or the prior knowledge which is required, determine the ECM effectiveness, but it has been shown that even with very limited data the effectiveness is not degraded too much.
In many cases, the general type of the missile can serve as a basis for a rough parameter estimation. For example, a long-range missile can generally be associated with a certain range of weights and thus with its appropriate time constants. Some prior intelligence information, especially regarding T_{SW}, is always helpful and can save precious engagement time thus increasing the probability of obtaining a large miss. The dependence of the probability-density-function of the miss-distance on the combined prior and real-time data should be further investigated.

Most of the work reported here was concerned with only a particular ECM method (circular orbit). More work should be done regarding other types of ECM such as gain-switching (which is a 1-D method and thus needs synchronization with respect to the collision time).

The application and extension of this work to the case of anti-ship missiles also seems to be a very important subject in our future work.

REFERENCES

1. "Classical and Modern Guidance of Homing Interceptor Missiles," David [illegible] Leland, a presentation to the seminar of Dept. of Aeronautics and Astronautics, MIT, Cambridge, Massachusetts, April [illegible]

2. Random Processes in Automatic Control, J. Laning and R. Battin, McGraw-Hill, New York, 1956.

3. "Application of Computer Techniques to Evaluation of Complex Statistical Functions," J. Pfaffer and R. Favreau, a presentation to IRE National Convention, March 1956.

4. Linear Time-Varying Systems: Analysis and Synthesis, Henry D'Angelo, Allyn and Bacon, Boston 1970.

5. Linear Systems, Chapter 9, Thomas Kailath, Prentice-Hall, 1980.